Anomalies and Artifacts in Raman Spectroscopy

Bryan T. Bowie[1,4], D. Bruce Chase[2], Ian R. Lewis[3] and Peter R. Griffiths[1]

[1] *University of Idaho, Moscow, ID, USA*
[2] *E.I. du Pont de Nemours and Co., Inc., Wilmington, DE, USA*
[3] *Kaiser Optical Systems, Inc., Ann Arbor, MI, USA*
[4] *Current address: Thermo Nicolet, Madison, WI, USA*

1 INTRODUCTION

The feasibility of Raman spectroscopy was demonstrated by Raman and Krishnan in 1928 in their seminal article describing the discovery of 'A New Type of Secondary Radiation',[1] although it should be noted that it was not until 1929 that a spectrum was actually shown.[2] This report was the first experimental verification of what would become the effect now named in Raman's honor for which he received the Nobel Prize in Physics in 1930. It is noteworthy that the effect of polarization on these spectra was noted in this paper. Thus this paper was arguably the first report of the existence of possible instrumentally induced artifacts in Raman spectra. Because of the low sensitivity of the technique and the susceptibility of samples to fluoresce when illuminated with a beam of intense visible radiation, Raman spectrometers were largely to be found in the laboratories of a few specialists in this technique until the late 1980s.[3,4] Indeed fluorescence, because of the electronic spectrum of either the sample itself or (more commonly) trace impurities, was the biggest road-block to the acceptance of Raman spectroscopy as an instrumental technique that could be routinely used in the analytical chemistry laboratory. This situation changed in the mid 1980s, when it was shown that near-infrared (NIR) lasers could be used to complement the visible sources of monochromatic radiation that had always been used for Raman spectrometry excitation until that time. The use of NIR excitation to minimize sample fluorescence had not been feasible prior to this time for several reasons:

- Photomultiplier detectors had poor response at longer wavelengths than ~800 nm.
- The Raman cross-section of bands is approximately proportional to the fourth power of the wavenumber of the Raman-scattered radiation, so that visible radiation sources gave much greater Raman cross-sections than NIR sources.
- Multiplex techniques, and in particular Fourier transform (FT)-Raman spectroscopy, were precluded because of the shot noise caused by the intense Rayleigh line.

In the mid-1980s, a number of technological breakthroughs led to the development of NIR Raman spectrometers and hence to the popularity of Raman spectroscopy today. First, the development of highly efficient laser-line blocking filters allowed Rayleigh-scattered radiation to be blocked before reaching the detector, thereby minimizing the effect of photon shot noise. This was the single most important factor leading to the development of FT-Raman spectrometers with 1064-nm excitation from an Nd : YAG laser and germanium or indium gallium arsenide (InGaAs) detection[5,6] but was also important for dispersive Raman spectrometers. Shortly after the commercial introduction of FT-Raman spectrometers, polychromators with charge-coupled device (CCD) array detection were also introduced for NIR Raman spectroscopy.[7–9] The key technological innovations leading to the development of these instruments were the development of 785-nm and 840-nm diode lasers,[10–12] polychromators based on both reflective and transmissive holographically recorded gratings[13,14] and, as noted above, laser-line blocking filters. These filters, starting initially with long-pass dielectric filters[3] and more

Handbook of Vibrational Spectroscopy, Online © 2006 John Wiley & Sons, Ltd.

This article was published in the *Handbook of Vibrational Spectroscopy* in 2006 by John Wiley & Sons, Ltd.
DOI: 10.1002/9780470027325.s3103

recently holographic notch filters,[14,15] as described in this Handbook by Owen (**Volume Phase Holographic Optical Elements**), enabled the second and third monochromators of earlier Raman spectrometers to be eliminated. The development of small high-power visible lasers, especially those based on the frequency-doubled line from the Nd : YAG laser at 532 nm,[16,17] has further increased the popularity of Raman spectroscopy for the study of samples that do not fluoresce at this wavelength.

Raman spectrometry is a particularly attractive technique for vibrational spectroscopy because little or no sample preparation is usually required. As a result of the technological breakthroughs that were made in the 1980s, Raman spectrometers are now being used for more routine qualitative and quantitative measurements than ever before and Raman spectroscopy has become more popular than at any other time in its 70-year history. Many users of Raman spectrometers have had some experience in vibrational spectroscopy working with Fourier transform infrared (FT-IR) spectrometers. It is, therefore, to be expected that these spectroscopists want to be able to process Raman spectra in the same way that they process infrared spectra, applying such techniques as ordinate expansion and spectral subtraction for the study of weak bands due to minor components or small band shifts that give indications of physical effects such as phase changes. Recently, tests have been described that are designed to reveal the presence of weak artifacts and anomalies in FT-IR spectra.[18,19] There is a need for similar types of investigations to be carried out with Raman spectrometers. In this article, we discuss many of the factors that can lead to the generation of anomalies and artifacts in Raman spectra measured on contemporary instruments.

2 INSTRUMENTAL EFFECTS

In this section some of the many environmental factors that can affect measurements on a Raman spectrometer will be discussed. These include effects due to the instrument and the ambient conditions, such as temperature variations and room lighting. One factor which will not be considered in depth, but which could lead to erroneous results, is vibration. For example a Raman microscope is often employed to study samples which cannot be examined by IR microscopy since they are smaller than the IR diffraction limit. In the case of a Raman microscope, operating with diffraction-limited focusing performance on a diffraction limited sample in a matrix, vibration of the sample may cause the Raman microscope to actually collect a spectrum of both the sample and the matrix. The resulting spectrum truly represents the sample presented to the instrument for the measurement period but the resultant spectrum does not represent what the technique is capable of producing. Thus the sample spectrum is contaminated by an artifact (the matrix spectrum), which originates neither from the instrument nor the sample themselves but from poor experimental design.

2.1 Laser output

The laser itself can be the source of additional artifacts. In Raman spectroscopy, Raman bands appear shifted from the source laser line. If the source is not monochromatic then extra lines will appear in the spectrum (this holds true irrespective of the spectrometer type). For example, both flashlamp-pumped and diode-pumped Nd : YAG lasers exhibit additional nonlasing emission lines which must be optically filtered or they can interfere with the Raman spectrum. In the case of an FT-Raman spectrometer, these lines will yield additional features in the spectrum and additional shot noise distributed across the whole spectrum.

In the case of dispersive Raman spectroscopy using 785-nm excitation from either a Ti : sapphire or a diode laser, both spontaneous and stimulated radiation may be emitted from the laser head. In the case of the Ti : sapphire laser additional lines may appear which originate from the pump laser. Spontaneous emission, if not filtered, may appear in the spectrum as a broad background at low Raman shift values.

With appropriate optical filtering of the laser output using bandpass filters (such as dielectric interference or holographic) or a grating monochromator, this type of artifact can be removed.

2.2 Filter effects

If the spectrometer is illuminated with a sample which luminesces then a profile of the laser-line blocking filter will be observed superimposed on the sample spectrum. Depending on the filter type, either dielectric or holographic, the filter profile may be seen throughout the spectrum in the case of dielectric filters[20] or restricted to the low frequency region of the spectrum between 100 and 400 cm^{-1} shift (see **Volume Phase Holographic Optical Elements**). This type of artifact may be completely removed by calibrating the intensity axis of the spectrometer (see **Photometric Standards for Raman Spectroscopy**).

2.3 Shifts in the wavenumber scale

It is well known that FT-IR spectra can exhibit small wavenumber shifts caused by vignetting,[21] i.e. changing

Handbook of Vibrational Spectroscopy, Online © 2006 John Wiley & Sons, Ltd.

This article was published in the *Handbook of Vibrational Spectroscopy* in 2006 by John Wiley & Sons, Ltd.
DOI: 10.1002/9780470027325.s3103

or moving the limiting aperture of the instrument. These shifts are rarely more than a few tenths of the resolution at which the spectrum is being measured. Nonetheless, if spectra measured before and after changing the limiting aperture are subtracted, the difference spectrum has the appearance of the first derivative of the spectrum. Similar results are seen in FT-Raman spectrometry where the limiting aperture is the emission area of the sample itself. Currently FT-Raman spectrometers that use either reflective or refractive collection optics are commercially available. A refractive collection optic, in terms of signal collection, has been shown to be much less sensitive to sample alignment than its reflective counterpart.[20] The FT-Raman spectrum of cyclohexane, which is a strong Raman scatterer with several narrow bands, is shown in Figure 1(a). The result of subtracting two spectra of cyclohexane, acquired sequentially, is shown in Figure 1(b). The reproducibility of the wavenumber scale is so good that no trace of any artifacts is seen in the difference spectrum. The cell was then removed from the sample holder and replaced, and its position adjusted to give rise to the most intense spectrum. After subtracting this spectrum from one of the spectra acquired before sample repositioning, the amplitude of the features in the difference spectrum found on applying an "auto-subtraction" routine is significantly greater than the noise, as shown in Figure 1(c). The sharper bands in the spectrum appear as derivative-shaped peaks due to a small shift in the effective position of the limiting aperture. Other bands appear with a negative bias, indicating that the subtraction process cannot effectively compensate for changes in intensity due to slightly different collection efficiency. Similar results have been reported for anthracene by Parker *et al*.[22] Effects such as these would reduce the quantitative accuracy of FT-Raman spectrometry.

For an interferometer, high accuracy of the wavenumber scale is claimed because of the use of an internal helium–neon (He–Ne) laser that permits the interferogram to be sampled at equal intervals of retardation.[21] However if the He–Ne laser is misaligned, or realigned inappropriately when an instrument is serviced, a small linear wavenumber shift will be introduced. Since it is linear with wavenumber, this shift is easily corrected, and the precision of the instrument remains unaffected. However the accuracy of the instrument would be compromised.

CCD-Raman spectrometers are more susceptible to shifts in the abscissa scale because the wavenumber of spectra measured using this type of instrument are not referenced to the wavenumber of an He–Ne laser as they are in FT-Raman spectrometers. Whereas the wavenumber scale of an FT-Raman spectrometer is relatively immune to changes in ambient temperature, this is not the case for a CCD-Raman spectrometer, where shifts of at least $0.05\,cm^{-1}\,°C^{-1}$ are not uncommon for certain spectrometer types. The spectrum of acetonitrile measured on a CCD-Raman spectrometer is shown in Figure 2(a). After removing the sample, replacing it and refocusing the beam, the residual features in the difference spectrum were actually smaller than they were with the FT-Raman spectrometer (Figure 2b). This is easily explained by the fact that changes in sample position for a dispersive instrument will only change the flux through the instrument as focusing on the slit is changed. To first order, this does not produce a frequency shift. The subtraction process can effectively correct for changes in spectral

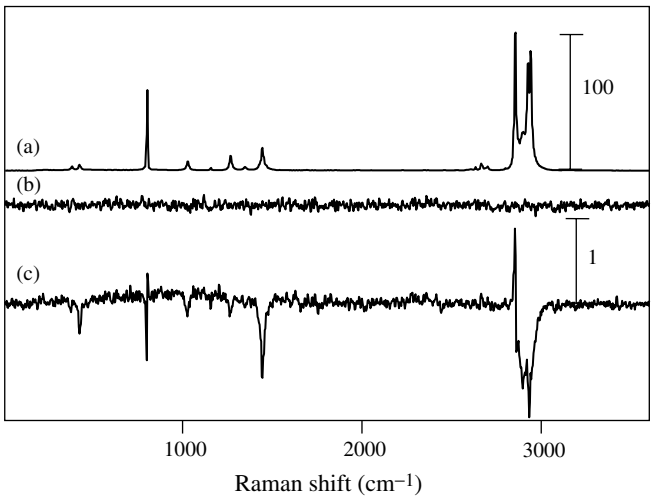

Figure 1. Result of subtracting two spectra of cyclohexane measured on an FT-Raman spectrometer. (a) Spectrum of cyclohexane; (b) result of subtracting two successive spectra of cyclohexane; (c) result of subtracting two spectra of cyclohexane taken before and after refocusing the beam at the sample.

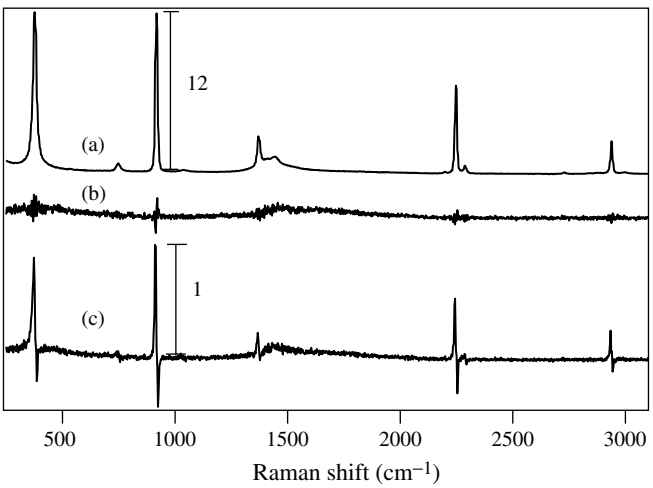

Figure 2. Result of subtracting spectra of acetonitrile spectra measured on a CCD-Raman spectrometer. (a) Spectrum of acetonitrile; (b) result of subtracting two spectra of acetonitrile taken before and after refocusing the sample; (c) result of subtracting two spectra of acetonitrile taken 10 h apart with the sample in the same position.

Handbook of Vibrational Spectroscopy, Online © 2006 John Wiley & Sons, Ltd.

This article was published in the *Handbook of Vibrational Spectroscopy* in 2006 by John Wiley & Sons, Ltd.
DOI: 10.1002/9780470027325.s3103

intensity across the entire spectrum. On remeasuring the spectrum 10 h later and subtracting this spectrum from the one measured earlier in the day, however, large derivative features, caused by drift of the monochromator with temperature, are apparent in the difference spectrum, as shown in Figure 2(c). These features are not a result of sample heating, which generally causes bands to broaden. In the event of sample heating, the features in the difference spectrum generally have the appearance of the second derivative rather than the first derivative that results from a spectral shift.

In dispersive Raman spectroscopy, in order to address wavelength calibration concerns, several commercial instruments have been developed[23,24] which incorporate atomic line sources into the spectrometer to allow either simultaneous or near-simultaneous measurement of both the Raman spectrum of the sample and atomic emission lines from the lamp. In all cases a sub-detector element mapping calibration is performed.[25,26] A high order polynomial fitted to the emission lines is used to generate a pixel-by-pixel calibration. This calibration provides primary wavelength calibration of the dispersive Raman spectrometer. The use of an incorporated calibration source allows the user to perform either on-the-fly push button calibration or automated calibration at specific time intervals. Another approach for automated calibration of dispersive Raman instruments has been proposed by Carman *et al*.[27]

After establishing that the primary wavelength calibration of the instrument is correct, the final question for wavenumber accuracy of the Raman spectrum is the position of the laser line. In all Raman spectrometers the laser wavelength is used to calculate the Raman shift values. Ideally the laser wavelength could be provided to the system software only once and the wavelength would remain stable. Unfortunately in practice this is not the case.

All lasers will shift their lasing wavelengths to a greater or lesser degree as the environmental temperature changes. Both frequency-doubled Nd : YAG (532-nm) and 1064-nm Nd : YAG lasers have been shown to shift their lasing wavelengths by up to $0.1\,\mathrm{nm}\,^{\circ}\mathrm{C}^{-1}$.[28] A shift between the stored laser wavelength and the actual laser wavelength will cause a linear shift in the measured wavenumber of Raman bands.

In dispersive Raman spectroscopy the spectrometer can either scan over the laser line to observe the actual laser wavelength and this value can be updated in the Raman shift calculation or a small amount of the laser line can be picked-off and directed onto the CCD detector during the data acquisition.[23]

In FT-Raman spectroscopy the laser is often totally blocked by laser-line rejection filters and thus direct observation of the laser line may not be possible. For FT-Raman spectrometers two approaches are available for checking the laser wavelength and back-calculating its position if necessary:

1. For all FT-Raman spectrometers, a Raman standard can be used (**Wavenumber Standards for Raman Spectrometry**) and the user can check to see if the measured peak positions correspond with the published values.
2. For FT-Raman spectrometers equipped with notch filters, any Raman sample can be used and the user checks the symmetry of the Stokes and anti-Stokes Raman bands. Any difference in position between the anti-Stokes and Stokes can be assigned to an improper value of the laser wavelength.[29]

2.4 Aliasing

Aliasing occurs with FT spectrometers when the frequency of the sinusoidal wave associated with a particular spectral feature (or noise) is more than half the sampling frequency, i.e. when spectral features or noise are aliased around the Nyquist frequency. To minimize aliasing, the signal from the detector is usually delivered into low-pass electronic filters to attenuate signals above the Nyquist frequency. Generally speaking, aliasing is difficult to observe in a mid-infrared spectrum measured on an FT-IR spectrometer for two reasons. Firstly, it is common to sample the signal interferogram once per wavelength of the He–Ne laser interferogram, e.g. once per downward-going zero-crossing. For measurements taken in this way, the Nyquist frequency is usually $\sim 7900\,\mathrm{cm}^{-1}$, which is well above the highest wavenumber where the observed infrared intensity is nonzero. Furthermore, spectral features that did fold into the mid-infrared spectrum would be intrinsically very weak, since it would have to be derived from the low intensities observed above $7900\,\mathrm{cm}^{-1}$. On the other hand, FT-Raman spectra measured with a 1064-nm Nd^{3+} : YAG laser at $9395\,\mathrm{cm}^{-1}$ typically cover the range from about 9500 to $6000\,\mathrm{cm}^{-1}$ and the interferogram must be sampled every zero-crossing of the He–Ne laser interferogram, so that the Nyquist frequency is equal to the wavenumber of the He–Ne laser, or $\sim 15\,800\,\mathrm{cm}^{-1}$.

We have observed an unusual effect in FT-Raman spectrometry that must be attributed to a different type of aliasing. This effect will be illustrated with the spectrum of sulfur, which is shown in Figure 3(a). Sulfur has two strong bands at $218\,\mathrm{cm}^{-1}$ and $472\,\mathrm{cm}^{-1}$. Two very weak bands can be observed in the spectrum at $2515\,\mathrm{cm}^{-1}$ and $2769\,\mathrm{cm}^{-1}$. Although the $2769\,\mathrm{cm}^{-1}$ band is close enough to the C–H stretching region that one may initially assign it to a C–H stretch of some sort, the band at $2515\,\mathrm{cm}^{-1}$ cannot be easily assigned to any fundamental transition.

Handbook of Vibrational Spectroscopy, Online © 2006 John Wiley & Sons, Ltd.

This article was published in the *Handbook of Vibrational Spectroscopy* in 2006 by John Wiley & Sons, Ltd.
DOI: 10.1002/9780470027325.s3103

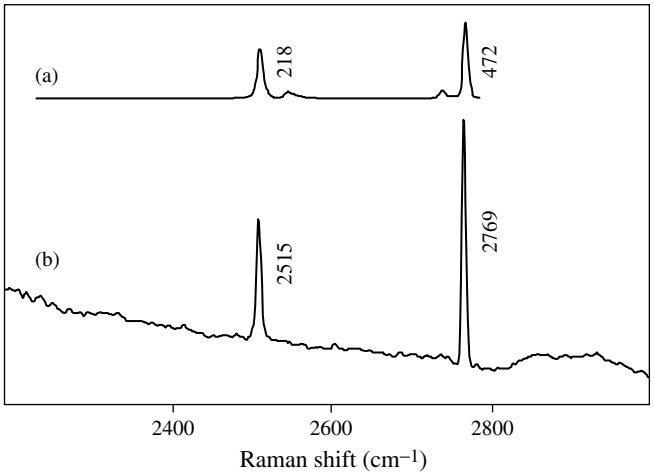

Figure 3. Aliasing about one-half the Nyquist frequency. (a) Spectrum of sulfur measured on an FT-Raman spectrometer; (b) the resultant bands of sulfur after folding about one-half the Nyquist frequency.

Table 1. Effect of aliasing about one-half the Nyquist frequency.

Vibrational frequency of sulfur bands (cm^{-1})	219	473
Absolute wavenumber of Raman band	9176	8922
Wavenumber after folding about 7901 cm^{-1}	6626	6880
Apparent Raman shift	2769	2515

In fact, both these bands are caused by a type of aliasing of the strong sulfur bands at 218 and 472 cm^{-1}. The absolute wavenumber of these bands is 9176 and 8922 cm^{-1}, respectively. If they were folded about 7901 cm^{-1} (one-half of the Nyquist frequency), they would appear at 6626 and 6880 cm^{-1}. On subtracting these frequencies from 9395 cm^{-1}, the laser frequency, they would appear at Raman shifted wavenumbers of 2769 and 2515 cm^{-1}, which is within 1 cm^{-1} of the wavenumber at which they are measured. This is summarized in Table 1. The aliasing effect seen here is probably caused by the He–Ne laser interferogram not being exactly sinusoidal in the spectrometer being used for this measurement. Thus there could be a small difference in this distance between an upward- and a downward-going zero crossing and a downward and an upward-going zero-crossing that could lead to this type of artifact.

2.5 Multi-passing errors

Another artifact that we have observed in FT-Raman spectra is almost certainly caused by radiation from the sample being reflected back into the interferometer by an optical component (probably one of the filters). This radiation would be modulated a second time by the interferometer before reaching the detector. This effect is illustrated using diphenylethyne, the spectrum of which is shown in Figure 4(a). The C≡C stretching band of this molecule is at 2221 cm^{-1} and the aromatic C–H stretch is at 3064 cm^{-1}. Artifacts caused by double-modulation of these bands can be seen in the anti-Stokes Raman spectrum at 4953 cm^{-1} and 3267 cm^{-1}, as shown in Table 2.

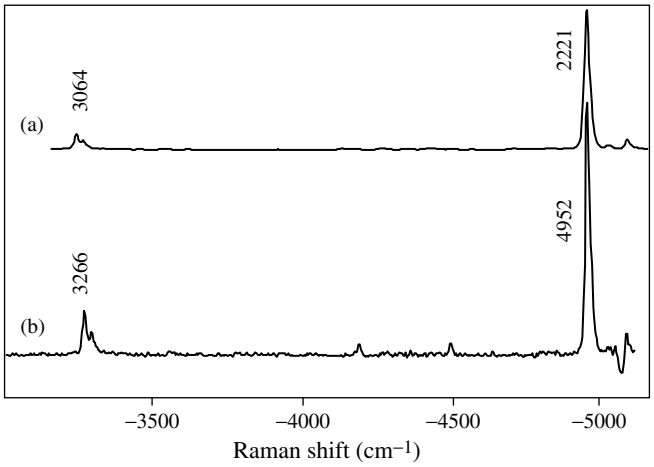

Figure 4. Frequency doubling in FT-Raman caused by double modulation. (a) FT-Raman spectrum of diphenylethyne; (b) the frequency doubled spectrum.

Table 2. Effect of frequency doubling of FT-Raman spectra.

Vibrational frequency of diphenylethyne bands (cm^{-1})	3064	2221
Absolute wavenumber of Raman band	6331	7174
Wavenumber after folding about 7901 cm^{-1}	12 662	14 348
Apparent Raman shift	−3267	−4953

2.6 Detector effects

Several artifacts/anomalies can be traced back to the detector as the origin. These include:

- wavelength sensitivity
- "etaloning"
- pixel-to-pixel variation (Section 2.7)
- dark noise (Section 2.8)
- hot pixel and cosmic rays (Section 2.9)
- charge traps
- column defects.

Handbook of Vibrational Spectroscopy, Online © 2006 John Wiley & Sons, Ltd.

This article was published in the *Handbook of Vibrational Spectroscopy* in 2006 by John Wiley & Sons, Ltd.
DOI: 10.1002/9780470027325.s3103

All of the items listed above may be observed with a CCD-Raman spectrometer while only wavelength sensitivity is of concern in FT-Raman spectroscopy.

The CCD-detector used in dispersive Raman spectroscopy is a multi-element array of individual detector elements. In a typical 1024 × 256 array there are over 250 000 individual detector elements. The manufacturers of these devices attempt to limit the difference between the individual elements at the 1–3% level but even this difference can be significant for a weak signal, such as a Raman spectrum. A number of these effects (pixel-to-pixel variation, dark noise and hot pixels) are described in greater detail below. Effects such as etaloning, charge traps, and column defects have been described in the literature.[30] These effects can appear in the spectrum if the spectrometer is not intensity corrected.

In both CCD- and FT-Raman spectrometers if either the excitation wavelength or the actual spectrometer type is changed, then the measured spectrum will show different relative intensities for the same sample. For example if the Raman spectrum excited with 532-nm excitation is compared to that recorded with 785-nm excitation then suppression of long wavelength (high Raman shift) bands with 785-nm is observed. This artifact can be traced back to the detector quantum efficiency (QE) curve (sensitivity at each wavelength). The QE of the detector can be a significant contributor to the overall response function of the spectrometer. Fortunately calibration of the intensity axis of the spectrometer will effectively correct for this artifact. (see **Photometric Standards for Raman Spectroscopy**).

2.7 Noise effects

When there is a large photon flux incident on visible and NIR detectors, the noise level on their output is increased by photon shot noise. Indeed, had laser-line rejection filters not been designed to reduce the amplitude of the Rayleigh line below that of the stronger Raman bands, FT-Raman spectrometry would not have become a viable technique, since shot noise associated with the extremely strong Rayleigh line would be distributed throughout the entire spectrum. Even strong Raman lines can increase the noise in FT-Raman spectra, as can be seen from the spectra shown in Figure 5. Each of these traces is the difference between two sequentially measured spectra in regions where the samples (if any) have no fundamental bands. The difference between two spectra measured with the laser switched off is shown in Figure 5(a); the noise level in this trace represents the intrinsic detector noise in the absence of signal. When the corresponding spectrum is measured with the laser on and with cyclohexane in the cell, the noise level is approximately doubled (see Figure 5b). Cyclohexane has a fairly high, but not exceptionally large, Raman cross-section. When a very strong Raman scatterer, such as methyl styryl benzene (MSB), is placed in the sample cell, the noise level is dramatically increased, see Figure 5(c). This situation is exacerbated when samples fluoresce strongly, as fluorescence is usually of higher integrated intensity than Raman-scattered radiation and present over a wide spectral region. Assuming that the noise in Figure 5(b) and 5(c) is largely the result of shot noise, it should increase with the square root of the laser power as discussed first by Hirschfeld.[31] This is indeed the case as shown in Figure 6. This result produces the interesting effect that further improvements in detector performance will not improve the signal-to-noise ratio (S/N) of spectra

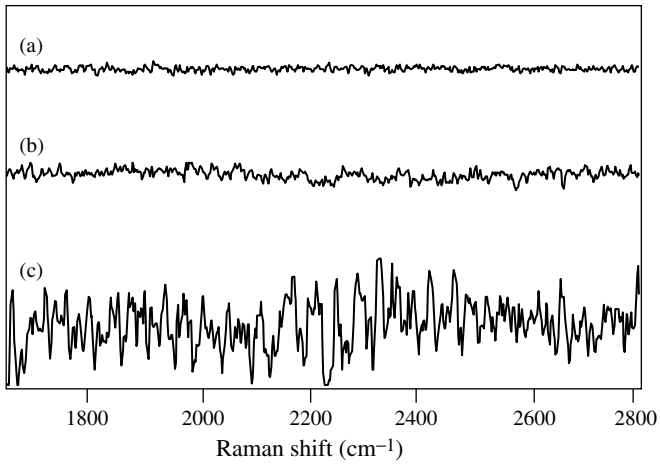

Figure 5. Shot noise in FT-Raman spectrometry. (a) Noise with the laser turned off; (b) noise of an FT-Raman spectrum of cyclohexane (C_6H_{12}); (c) noise of an FT-Raman spectrum of MSB collected at the same laser intensity as the cyclohexane sample.

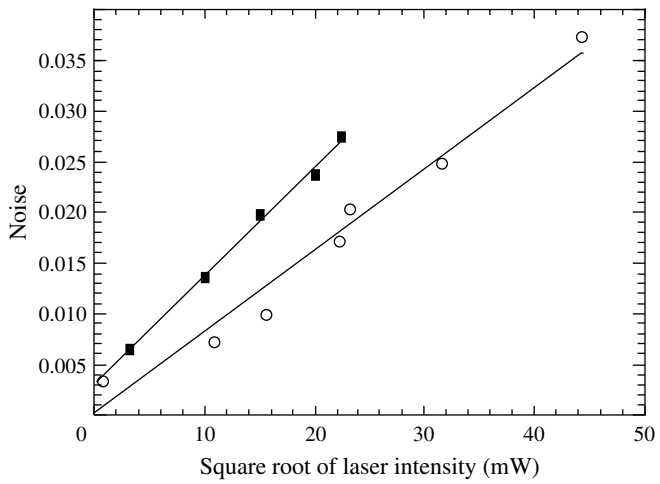

Figure 6. Root mean square noise of baseline regions in the spectra of cyclohexane and MSB versus the square root of the laser intensity.

Handbook of Vibrational Spectroscopy, Online © 2006 John Wiley & Sons, Ltd.

This article was published in the *Handbook of Vibrational Spectroscopy* in 2006 by John Wiley & Sons, Ltd.
DOI: 10.1002/9780470027325.s3103

of strong scatterers. However, weakly scattering samples would benefit from reduced detector noise.

CCD detectors are also shot noise limited, and shot noise can be a bigger problem with CCD Raman spectrometry than with FT-Raman spectrometry because fluorescence is more commonly encountered in CCD-Raman spectra due to the shorter laser wavelength. The biggest difference between FT-Raman and CCD-Raman spectrometry in this respect is that shot noise is not distributed across the spectrum by CCD detectors, since the signal at each pixel is a function only of the intensity at that wavelength. The effect of shot noise became very evident when we attempted to measure the Raman spectrum of a polyimide (Kapton®) with a 785-nm laser. In this case, the spectrum was dominated by fluorescence (Figure 7a). A difference spectrum obtained from sequential acquisitions is shown in Figure 7(b), where it can be seen that the noise is strongly dependent on the signal at each pixel.

The effect of pixel-to-pixel variation can also lead to a type of noise that increases when the sample fluoresces. The spectrum of a sample of polyimide powder is shown in Figure 8(a). It is quite difficult to discern any Raman bands over the fluorescence in this region of the spectrum. On correcting for the pixel-to-pixel variations in response, the Raman spectrum of the polyimide is far more easily distinguished (Figure 8b). A spectrum of the same sample measured with an FT-Raman spectrometer is shown in Figure 8(c). It can be seen that the noise on this spectrum is significantly higher than the noise on the pixel-corrected CCD-Raman spectrum seen in Figure 8(b), even though the laser power for the FT-Raman spectrum was almost an order of magnitude greater and the measurement times for the two spectra were approximately equal. These spectra further illustrate the well-known fact that

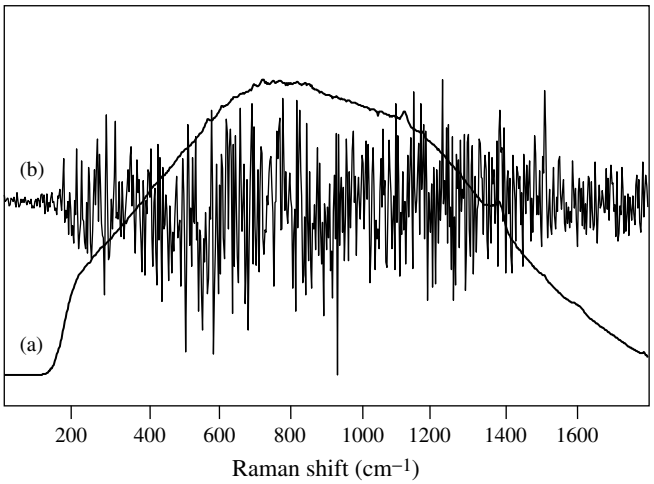

Figure 7. Shot noise of a CCD-Raman spectrometer. (a) CCD-Raman spectrum of Kapton®; (b) result of subtracting two successively acquired spectra of Kapton®.

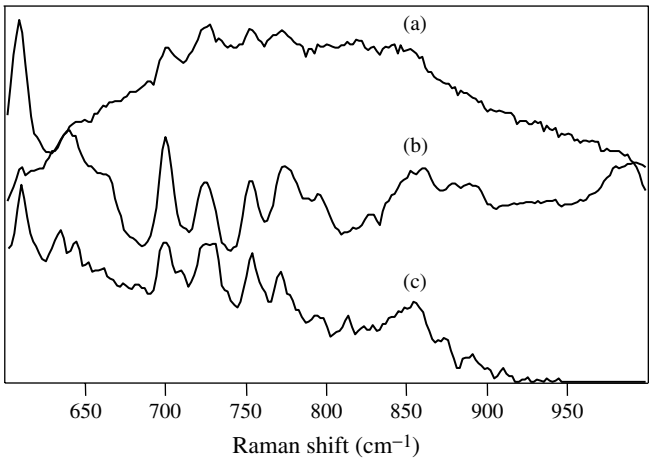

Figure 8. Pixel-to-pixel variation of CCD-Raman spectrometers. (a) CCD-Raman spectrum of a polyimide powder not corrected for pixel-to-pixel variations; (b) CCD-Raman spectrum of a polyimide powder corrected for pixel-to-pixel variations; (c) FT-Raman spectrum of the same polyimide powder.

CCD-Raman spectrometry is usually more sensitive than FT-Raman spectrometry except for those samples that fluoresce strongly when illuminated with laser radiation of shorter wavelength than 1064 nm. It should be noted that several workers have tried to quantify the sensitivity difference between FT- and CCD-based Raman spectrometers. An absolute measure which can be used to generalize on this subject is difficult to obtain, however, since the sensitivity difference will be a combination of instrumental, sampling, and sample effects.

2.8 Dark noise

The high sensitivity of CCD detectors can be partially lost because of other types of noise, especially dark noise. The noise level of CCD detectors is strongly dependent, not only on the temperature of the detector elements themselves, but also on the temperature of the readout electronics such as the shift registers, summing well and readout amplifier. The dark noise from a CCD detector is proportional to the square root of the temperature (in Kelvin) and is dependent on the frequency at which the CCD is read. The nonrandom dark noise is independent of the signal level and can be minimized by subtracting a spectrum measured by blocking the beam before it reaches the detector.[32] To illustrate the effect of dark noise on the sensitivity, the Raman spectrum of acetonitrile measured by averaging 50 scans using a detector that had been thermoelectrically cooled to −40 °C is shown in Figure 9(a). An expanded region of the spectrum measured without subtracting the dark spectrum is shown in Figure 9(b). The high noise level of this spectrum is readily apparent. The spectrum that

Handbook of Vibrational Spectroscopy, Online © 2006 John Wiley & Sons, Ltd.

This article was published in the *Handbook of Vibrational Spectroscopy* in 2006 by John Wiley & Sons, Ltd.
DOI: 10.1002/9780470027325.s3103

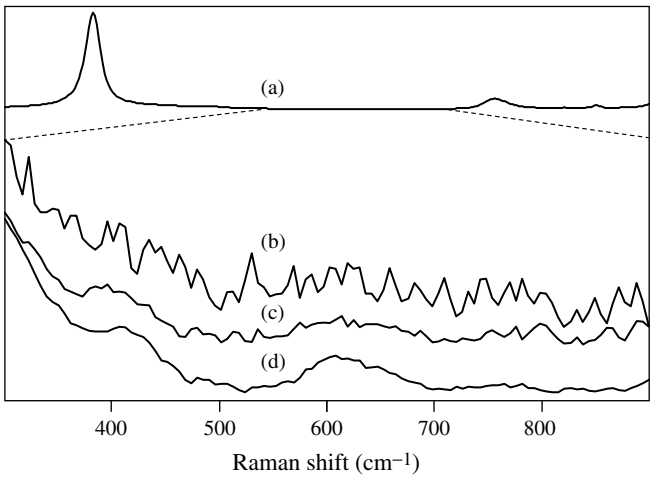

Figure 9. Dark noise of a CCD detector that was thermoelectrically cooled to −40 °C. (a) CCD-Raman spectrum of acetonitrile resulting from 50 coadded spectra; (b) a small region of this spectrum; (c) the same region after one dark noise scan was subtracted from the 50-scan spectrum; (d) the same region after 50 dark noise scans were subtracted from the 50-scan spectrum. Note that (b), (c) and (d) are all plotted on the same scale.

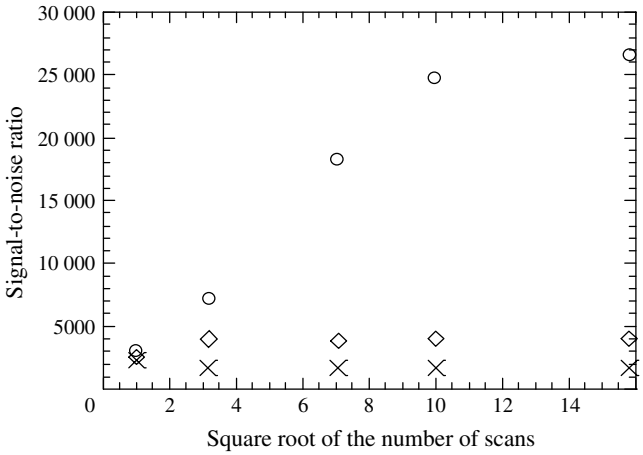

Figure 10. S/N of acetonitrile versus the square root of the number of scans, showing the degradation due to dark noise of a CCD detector. (○) The resulting S/N after subtracting a equal number of dark scans after coaddition; (×) the resulting S/N if no dark noise spectra were subtracted; (◊) the resulting S/N if only one dark noise spectrum was subtracted from the coadded spectra.

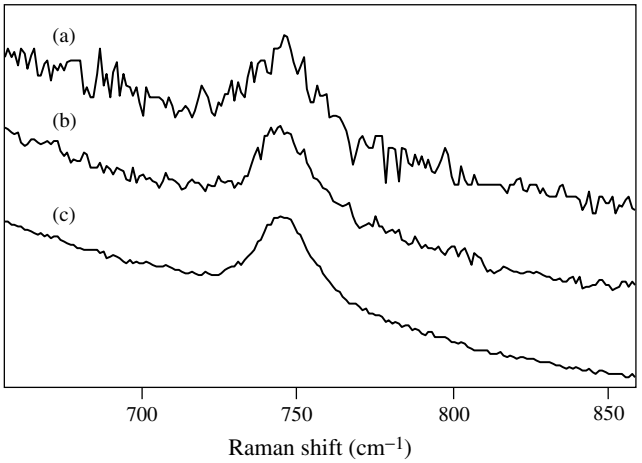

Figure 11. Raman spectrum of acetonitrile collected on a CCD thermoelectrically cooled to −70 °C. (a) The resulting spectrum after one accumulation; (b) the resulting spectrum after 10 accumulations; (c) the resulting spectrum after 100 accumulations.

resulted after subtracting a single dark scan is shown in Figure 9(c). It is apparent that the noise is much lower than that of the spectrum in Figure 9(b). If the dark spectrum measured with 50 scans is subtracted from the spectrum in Figure 9(b), the S/N is even higher (Figure 9d).

To investigate this effect more quantitatively, the S/N was calculated as the ratio of the peak height of the 920-cm^{-1} band of CH_3CN to the root-mean-square noise in the spectrum from 700 to 800 cm^{-1}. If the noise were truly random, a plot of the S/N against the square root of the number of scans averaged would be linear. The actual data are plotted in Figure 10. For spectra measured without subtracting a dark spectrum, the S/N does not change as the number of scans is increased. A similar result is found if the dark spectrum measured with a single scan is subtracted. On the other hand, when a dark spectrum measured with an equal number of scans is subtracted from the sample spectrum, the S/N increases linearly with the square root of the number of scans. The purpose of this dark subtraction is to remove a fixed pattern noise that is introduced by the detector even when no light is falling on the elements. The necessity of acquiring an equivalent number of dark scans is to ensure that the resultant spectrum is not dominated by the random dark noise obtained with a single scan. This is similar to the case for FT-IR spectrometry where one would always acquire a background spectrum at an equivalent or better noise level as the sample spectrum.

The cost of subtracting "dark noise" from the sample spectrum is that the measurement time is effectively doubled over the case where no dark subtraction is done. The dark noise shown here could be due to the effect of improperly cooling the CCD. A CCD chip that was cooled to −70 °C did not show any signs of dark noise dominance in the spectrum (Figure 11). However, it is possible that this effect may not be removed by simply lowering the temperature of the CCD since other CCD detectors cooled to only −40 °C have demonstrated that they too are not dark noise limited. Therefore, the dark noise may be caused either by improperly cooling the CCD or its read-out electronics. To further elucidate the effect of improper cooling of the CCD and its read-out electronics, the temperature of a liquid-nitrogen cooled CCD was raised from −70 °C to −40 °C while maintaining the same read-out frequency. This CCD exhibited no systematic dark noise at −70 °C, but showed systematic dark noise at the higher temperature.

Handbook of Vibrational Spectroscopy, Online © 2006 John Wiley & Sons, Ltd.

This article was published in the *Handbook of Vibrational Spectroscopy* in 2006 by John Wiley & Sons, Ltd.
DOI: 10.1002/9780470027325.s3103

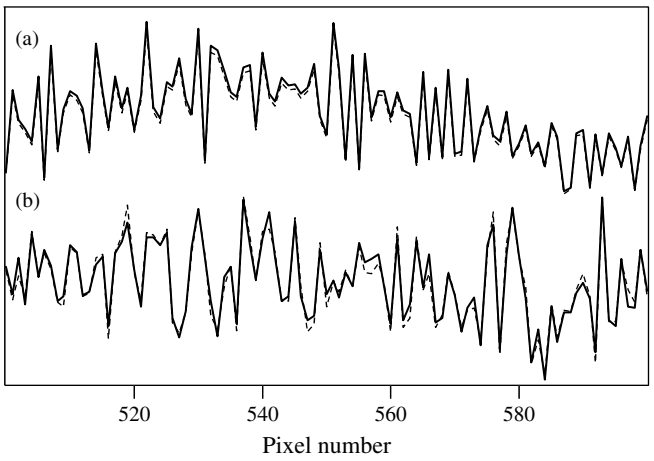

Figure 12. Dark noise and high intensity noise on a liquid nitrogen cooled CCD with its temperature set to −40 °C. (a) Repeat spectra of a white light source (solid and dashed lines); (b) repeat dark scans (solid and dashed lines).

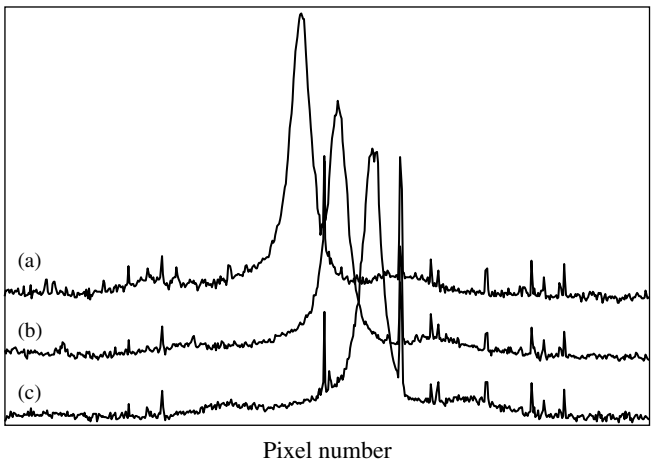

Figure 13. Effect of hot pixels. (a) CCD-Raman spectrum of sodium acetate; (b) spectrum of sodium acetate measured with grating center shifted by 20 cm^{-1}; (c) same spectrum measured with grating center shifted by 40 cm^{-1}.

Two sets of dark-noise spectra from this CCD at −40 °C were taken and overlaid on top of each other (Figure 12a). It is quite clear that at this temperature there is a fixed-pattern dark noise, which must be corrected by dark subtraction. To minimize dark noise, therefore, the entire chip and its readout electronics must be cooled and the correct read-out frequency corresponding to this temperature must be maintained. Also shown in Figure 12 are two overlaid spectra of a white light source. The white light source shows systematic errors different from the dark scans. Thus, it is plausible that the systematic or fixed noise pattern is dependent on the intensity of the incident radiation.

It should be noted that the results reported here should be extendable to a variety of CCD devices but the exact temperatures which show the effect may be dependent on chip type, architecture, size, read-out rate, etc.

2.9 "Hot pixels" and cosmic rays

Sometimes the response, or QE, of a certain pixel or row of pixels in a CCD array detector can be significantly higher than its neighbors. Such pixels are known as "hot pixels." In Raman spectrometry, hot pixels can lead to the appearance of sharp spikes in the spectrum. Three spectra of sodium acetate that were measured in the C-H stretching region are shown in Figure 13. For the upper spectrum the grating was centered at a Raman shift of 2950 cm^{-1} and held stationary. Approximately 100 pixels perpendicular to the wavenumber axis were binned and the spectrum was collected for 2 min; 10 such spectra were signal averaged. The middle and lower spectra were measured in the same way after centering the grating at 2930 cm^{-1} and 2910 cm^{-1}, respectively. It can be seen that the Raman spectrum shifts each time the grating is centered to a different wavenumber but the spikes remain in the same place. After reducing the number of pixels binned perpendicular to the wavenumber axis, the sharp spikes were eliminated.

Another source of sharp spikes in the spectrum is low-level radiation events that are commonly referred to as cosmic rays. Cosmic rays can, in principle, be observed with both FT- and CCD-Raman spectrometers. Unlike the case for hot pixels, low-level radiation events are manifested randomly at different positions across the spectrum and are not predictable. The spectrum of acetonitrile measured with a detector having hot pixels is overlaid with a dark noise spectrum in Figure 14. The hot pixels overlay with each other and the remaining spikes are caused by low-level radiation events. Several approaches for reducing the effect of cosmic rays have been proposed.[33,34] These

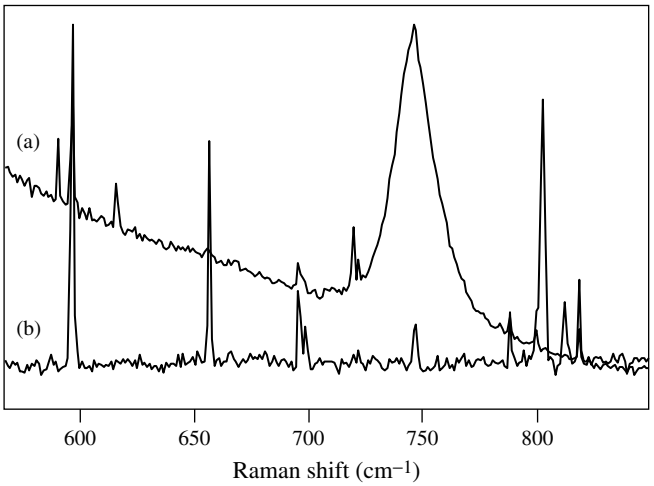

Figure 14. Hot pixels and cosmic rays. (a) CCD-Raman spectrum of acetonitrile; (b) dark noise scan.

Handbook of Vibrational Spectroscopy, Online © 2006 John Wiley & Sons, Ltd.

This article was published in the *Handbook of Vibrational Spectroscopy* in 2006 by John Wiley & Sons, Ltd.
DOI: 10.1002/9780470027325.s3103

include spike removal by comparing sequentially measured spectra and eliminating the spikes that are not reproducible from one scan to the next, and reduction in spike intensity by measuring multiple spectra and averaging.

Cutler *et al.*,[35] from the FT-Raman development group at Perkin-Elmer (Beaconsfield, UK), described the problem of cosmic rays or "Muon interference" in their early work on FT-Raman with pulsed excitation. Cosmic rays despite being measured in FT-Raman experiments rarely appear as a problem to the user. This is because the cosmic ray leads to an intense spike being observed in the interferogram but not at the centerburst. These interferograms can be flagged as unacceptable by the instrument control software and the scan discarded. Under those conditions the spectrometer simply keeps collecting scans, and rejecting unacceptable scans until the user defined number of "good scans" has been measured. For example if 200 scans are requested 205 scans may need to be collected. The only anomaly evident to the users is that the spectral acquisition takes longer than expected. It should be noted that the optical scanning velocity of the interferometer is determined by the detector type and its response time characteristics. For one commercial FT-Raman spectrometer, currently available, each single scan takes 1 s with a germanium detector while a single scan with an InGasAs detector takes 7 s. Thus depending on the detector available and the type of measurement being attempted (static or kinetic) the effect of cosmic rays may be either unnoticeable or noticeable to the user.

2.10 Summary

While the performance of both FT-Raman and CCD-Raman spectrometers has improved greatly over the past 10 years, it is clear that each instrument has its own set of limitations. For example, CCD-Raman spectrometers can maintain better short-term wavelength reproducibility than FT-Raman spectrometers after the beam has been refocused on the sample. On the other hand, FT-Raman spectrometers can maintain stability over longer periods of time than their CCD counterparts as a result of laser fringe referencing. As the technology of dispersive Raman spectrometers has improved and built-in calibration devices have been incorporated into spectrometers, their capability to maintain both optical alignment and calibration over long periods of time has greatly improved.

FT-Raman systems can give rise to false bands as a result of aliasing and frequency doubling, although these bands may be quite weak. CCD-Raman systems can show sharp bands as a result of hot pixels or low-level radiation events. Most software offered by instrument manufacturers possess a function for elimination, or at least minimization, of the effects of low level radiation events from the spectrum originating from intense narrow spikes that are only one or two pixels wide. The occurrence of these events can greatly increase the measurement time if the frequency of the events is high. The software currently offered cannot do anything about hot pixels because they affect the spectrum on a continuous basis so that the height of the spikes increases with integration time. The effect of hot pixels can be eliminated by finding which pixels are most seriously affected and not reading them out. Flat-fielding, i.e. dividing the intensity at each wavenumber by the pixel response (found using an intensity correction source, see **Photometric Standards for Raman Spectroscopy**), will also minimize the effect of hot pixels. When the Raman bands are of low intensity, some CCD detectors can generate errors prohibiting signal averaging. These errors can be corrected by acquiring and subtracting spectra acquired while the beam is blocked. Thus, a different correction would need to be applied depending on the intensity of the spectrum.

In the absence of fluorescence, the intrinsic sensitivity of CCD-Raman spectrometers is typically at least an order of magnitude greater than that of FT-Raman spectrometers. However, all of these corrections add time to the measurement that can significantly reduce this advantage. Unfortunately, FT-Raman systems cannot regain this sensitivity by simply increasing the laser intensity by an order of magnitude. Because the noise is increased with the square root of the laser power, the laser power would need to be increased at least by two orders of magnitude. Ultimately, however, the choice of instrument for the new user will depend on the type of samples anticipated. An ideally equipped laboratory will have access to both FT-Raman and CCD-Raman spectrometers.

3 EFFECT OF SAMPLE

3.1 Introduction

NIR Raman spectroscopy is being increasingly used for the identification of organic and inorganic materials, microspectroscopy, characterizing the chemical and physical properties of polymers, process monitoring and quantification. In principle, after correction for the instrument response function, the nonresonant Raman spectrum of a given sample should be independent of the laser wavelength. However, for many samples, there are several factors that cause differences between Raman spectra measured with different wavelengths. In the previous section, we discussed artifacts that were found in Raman spectra that depended on the

Handbook of Vibrational Spectroscopy, Online © 2006 John Wiley & Sons, Ltd.

This article was published in the *Handbook of Vibrational Spectroscopy* in 2006 by John Wiley & Sons, Ltd.
DOI: 10.1002/9780470027325.s3103

type of spectrometer that was used for the measurement. In this section, we discuss several sample-dependent factors which may cause NIR Raman spectra to vary with the wavelength of the excitation laser. Before doing so, however, let us consider the factors that control whether the Raman spectrum of a given sample should be measured with a particular laser.

If the wavelength of the laser corresponds to an electronic transition of either the sample or an impurity, there is a strong possibility that fluorescence will occur. Indeed the main reason for the popularity of NIR Raman spectroscopy is the fact that there are so few compounds that have electronic energy states for which the difference in energy between the excited state and the ground state corresponds to a wavelength in the NIR. Obviously if the need to avoid fluorescence were the only factor, Raman spectroscopists would use a laser that has the longest possible wavelength. Since this is not the case in practice, we have to consider the factors that determine the intensity of a Raman spectrum measured with a particular laser.

The intensity of a band in the Raman spectrum of any compound measured with a quantum detector such as a CCD is given by

$$I_{\text{Raman}} \propto \sigma_v I_{\text{Laser}} \tilde{\nu}_{\text{Laser}} (\tilde{\nu}_{\text{Laser}} - \tilde{\nu}_{\text{Vib}})^3 \qquad (1)$$

where $\tilde{\nu}_{\text{Laser}}$ is the wavenumber of the laser, σ_v is the wavelength-independent Raman scattering cross-section for a particular vibrational transition at that wavenumber, I_{Laser} is the power of the laser, and $\tilde{\nu}_{\text{Vib}}$ is the wavenumber of the vibrational transition. $(\tilde{\nu}_{\text{Laser}} - \tilde{\nu}_{\text{Vib}})$ is the absolute wavenumber of the Raman band. The frequency-dependent term, $\tilde{\nu}_{\text{Laser}}(\tilde{\nu}_{\text{Laser}} - \tilde{\nu}_{\text{Vib}})^3$, which is often approximated as $(\tilde{\nu}_{\text{Laser}})^4$ represents the change in Raman scattering intensity which occurs when the laser frequency is changed. It also represents an effect on the relative intensities within a Raman spectrum as the Stokes shift increases. When comparing the Raman intensities between two supposedly identical spectrometers operating at different laser wavenumbers, the intensities should be corrected by the ratio of the respective terms:

$$\frac{\tilde{\nu}_{\text{Laser}(1)}(\tilde{\nu}_{\text{Laser}(1)} - \tilde{\nu}_{\text{Vib}})^3}{\tilde{\nu}_{\text{Laser}(2)}(\tilde{\nu}_{\text{Laser}(2)} - \tilde{\nu}_{\text{Vib}})^3} \qquad (2)$$

For example, let us consider a C=O stretching band at 1720 cm^{-1}, with excitation by the two most popular lasers for NIR Raman spectroscopy, the 1064-nm Nd : YAG laser and the 785-nm diode laser. The ratio of the $\tilde{\nu}_{\text{Laser}}(\tilde{\nu}_{\text{Laser}} - \tilde{\nu}_{\text{Vib}})^3$ terms is almost exactly a factor of 5 in favor of the 785-nm diode laser. One should remember that there are not the only wavelength-dependent effects on the Raman scattering intensity. The spectrometers themselves will have a wavelength dependence that may arise from grating or beamsplitter efficiencies, detector response and filter response. These effects should be corrected for in the normalization procedure. There is a final wavelength-dependent effect that also needs to be taken into account. FT-Raman spectrometers utilize detectors that are not quantum detectors, but power detectors. Since such detectors respond to power, the Raman intensities should be scaled by dividing by the absolute wavenumber throughout the Raman spectrum to correct for the lower power in a longer-wavelength photon.

Let us now consider the spectrometers that are used with each type of laser. The vast majority of measurements that are made with a 785-nm diode laser are made with a polychromator and CCD array detector. Because this is an array detector, the signals from all wavelengths are measured simultaneously throughout the acquisition of the spectrum, giving rise to the multichannel advantage over the corresponding measurement made with a single detector. Raman spectra excited with a 1064-nm Nd : YAG laser cannot be readily measured with a silicon-based CCD array because these detectors cut off very close to 1064 nm. Thus only the anti-Stokes Raman spectrum could be measured with a Nd : YAG laser and CCD detector. Instead, a Ge or InGaAs detector must be used, since the cut-off of these detectors is about 1670 nm (6000 cm^{-1}). Since the quality and availability of array detectors based on Ge or InGaAs is limited, FT spectrometers are almost always used for the measurement of Raman spectra with Nd : YAG lasers. The multiplex advantage of FT spectrometers over grating spectrometers equipped with a single detector is offset to some degree by the multichannel advantage of CCD Raman spectrometers. However, the sensitivity of thermoelectrically cooled silicon CCD array detectors is well over an order of magnitude higher than that of either Ge or InGaAs detectors. Thus again, there is a clear sensitivity advantage afforded by the use of a 785-nm laser in conjunction with a grating polychromator and CCD-array detector. It should be noted, however, that there have been several reports of the use of shorter excitation wavelengths with FT-Raman spectrometers.[36,37] However due to the simplicity and throughput of the CCD-based spectrometer and the difficulty in optimizing an FT-Raman spectrometer for operation from 12 800 to 6000 cm^{-1} (absolute), these instruments have remained largely research curiosities.

The principal advantage of the Nd : YAG laser for Raman spectroscopy is that its power can be increased to a level of over 1 W, whereas the power of most diode lasers does not exceed 200 mW. It is unusual to operate a Nd : YAG laser at such high power levels, however, as the effect of sample heating can be strongly detrimental, as will be shown later. We will now examine some of the effects of measuring different types of samples on these two types of Raman

Handbook of Vibrational Spectroscopy, Online © 2006 John Wiley & Sons, Ltd.

This article was published in the *Handbook of Vibrational Spectroscopy* in 2006 by John Wiley & Sons, Ltd.
DOI: 10.1002/9780470027325.s3103

spectrometer in more detail and illustrate these effects with practical examples.

3.2 Sample heating

When a laser is incident on a sample, the sample's thermal conductivity and the thermal conductivity of the surroundings can affect the absorption of the laser enough to increase the temperature of these samples. A sample can decompose, undergo a phase transition, or simply heat up and emit longer-wavelength radiation when it absorbs energy in this manner. The sample's electronic absorption spectrum has a strong effect on the probability that the sample will absorb enough radiation that it will heat up. Electronic transitions tend to be much weaker at longer wavelengths, although most black samples will absorb 1064-nm radiation quite strongly. On the other hand, many organic molecules have weak absorptions at this wavelength due to overtones or combinations of the fundamental transitions that absorb mid-infrared radiation. A hot sample emits black-body radiation, and the tail of the Planck curve extends well into the NIR for samples that are above 100 °C. When a Nd : YAG laser (lasing at 1064-nm) is used to measure Raman spectra, the absolute wavenumber range of the spectrum is between about 6000 and 9400 cm^{-1}. Not only is the black-body radiation strongest at 6000 cm^{-1} but the sensitivity of the Ge and InGaAs detectors is greatest near this wavenumber. Thus thermal interference to the Raman spectrum is greatest at the largest Raman shifts.

To illustrate the effect of sample heating, let us consider the following example. We were trying to obtain the FT-Raman spectrum of a sample of lightly reduced MoO_3, which is a white powder. The bands in the Raman spectrum of this compound are weak and so we tried increasing the laser power to increase the intensity of each spectral feature, as shown in equation (1). Representative spectra are shown in Figure 15. With a laser power of 20 mW, little effect of sample heating could be seen, but the spectrum was very weak (Figure 15a). On increasing the power to 40 mW, the intensity of the Raman bands doubled, but the baseline started to increase at high Raman shift because of the effect of sample heating (Figure 15b). When the laser power was increased to 150 mW (a typical power that is used for measuring the spectra of many colorless samples), the black-body radiation caused severe degradation of the spectrum (Figure 15c) as shown previously by Schrader *et al.*[38] The Raman bands in Figure 15(c) appear to be the same height as the bands in Figure 15(b). However, the ordinate scale of the spectrum in Figure 15(c) is compressed relative to that of the other two spectra. The S/N of the Raman bands in Figure 15(b) and 15(c) is about the same,

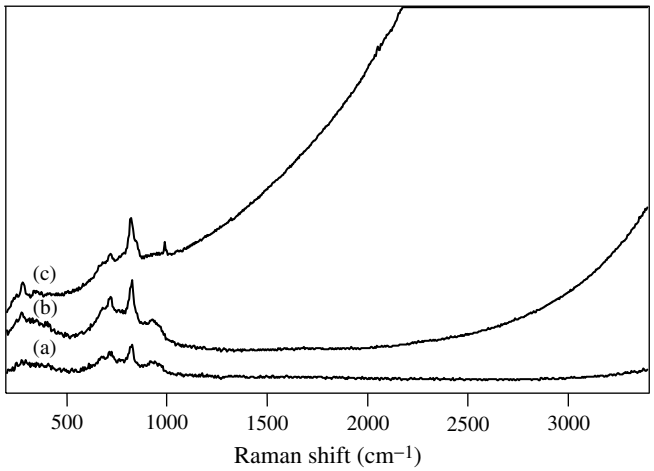

Figure 15. FT-Raman spectrum of MoO_3. (a) Laser power 20 mW; (b) laser power 40 mW; (c) laser power 150 mW.

because the thermal radiation has increased the shot noise in the spectrum.

In this case, another deleterious effect was observed. The heating due to the increased laser power slowly changed the structure of the sample. The Raman spectra between 200 and 1200 cm^{-1} are shown in Figure 16. The spectra measured with a laser power of 20 and 40 mW are essentially identical, with the S/N of the spectrum measured with a power of 20 mW being about half that of the spectrum measured at 40 mW. At 150 mW, the shape of the bands near 700 and 900 cm^{-1} Raman shift has changed and new bands are seen at ~275 and 1000 cm^{-1} shift, indicating a change in either the composition or crystal structure of the MoO_3 that results from the heating by the laser. Thus for samples that absorb radiation at the laser wavelength, however weakly, the operator must be careful to select the appropriate laser power to maximize the S/N and minimize black-body radiation caused by sample heating.

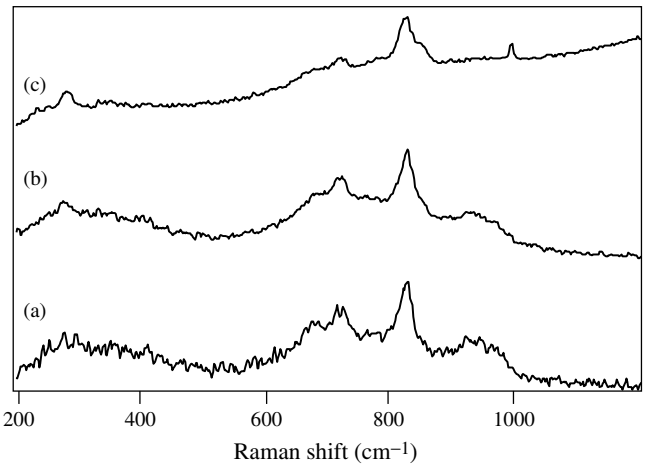

Figure 16. Expanded plot of Figure 15. (a) Laser power 20 mW; (b) laser power 40 mW; (c) laser power 150 mW.

DOI: 10.1002/9780470027325.s3103

Since, for spectra measured with a FT-Raman spectrometer equipped with a Nd : YAG laser, the intensity of the black-body radiation is relatively small at low Raman shift (around 9400 cm^{-1}), it might be thought that it may be better to measure the Raman spectrum of this sample with a CCD-Raman spectrometer equipped with an even shorter wavelength laser, such as a 785-nm diode laser. With this instrument, the Raman spectrum of interest would be located between absolute wavenumbers of about 12 800 and 11 800 cm^{-1} (although the spectrometer is capable of measuring spectra from absolute wavenumbers 12 800 (785-nm) to 9400 cm^{-1} (1064 nm)). When the MoO_3 sample was investigated with this instrument, however, the Raman spectrum could not be observed because of fluorescence.

A similar effect was seen by West while investigating $NaMnO_4$, which undergoes an irreversible phase transition at 112 °C.[39] The study by West also showed that changing the total time the laser is incident on the sample or the number of co-added scans can result in different spectra. This would be a direct result of the sample's heat capacity and/or the heat capacity of its surroundings.

Heating can also cause the widths of vibrational bands to increase. When two neighboring bands are unresolved, the center wavenumber of the resulting band can also change. These changes can cause errors in quantitative measurements. For example, the ratio of the Raman shifted bands of graphite at 1355 cm^{-1} (A_{1g}) and 1580 cm^{-1} (E_{2g}) is inversely proportional to crystal size. A study by Everall *et al*. showed that the effects of laser induced heating on graphite could cause false predictions about the graphite system being studied.[40] It was also demonstrated that the error increased as the laser spot size or particle size was decreased. The error increased as the size of the focused laser beam was reduced because of the increased energy density on the sample and the fact that there was less area accessible through which the heat could be conducted. The shape and intensity of the previously discussed bands as well as the first harmonic of the A_{1g} band at ~2700 cm^{-1} are known to vary with crystallinity even though their position is often used to determine the strain of a carbon fiber. In another study by Everall and Lumsdon,[41] consistent predictions of carbon fiber strain were demonstrated when the laser intensity was low while the results varied greatly when using high laser intensity.

Changes in bandwidth and band center as a function of temperature are also known to occur in liquids. Not only is this a concern for quantitative analysis but for proposed solid and liquid wavelength standards for Raman spectrometers. For example, cyclohexane is one of many proposed wavelength calibration standards and the effect temperature has on its bands had not been previously studied. Recently, however, the results of the effect of temperature (7–73 °C), as measured by the bulk temperature of a stirred solution, has on the Raman bands of cyclohexane has been published.[42] From this study, it was proposed that only certain bands in the spectrum should be used as a standard.

As mentioned above, a hot sample will emit enough thermal radiation that can overwhelm a Raman signal that is measured with 1064-nm excitation. Even relatively small changes in temperature can cause large changes in the spectrum. For example, the amount of thermal emission of an aqueous solution will increase by an order of magnitude for a 25 °C increase in temperature.[38] Some inorganic samples (e.g. MnO_2) will exhibit this effect with very low levels of excitation intensity making the collection of their Raman spectra impossible.

In Figure 17, the Raman spectrum of the wood, lodgepole pine, is shown.[43] The sample itself was a block of wood of approximate dimension 8 × 5 × 3 cm. The results of the Raman analysis using 1064-nm excitation are shown for different laser powers, 750 mW (Figure 17a) and 400 mW (Figure 17b). Figure 17(a) shows the familiar profile of a thermal background at high wavenumber. In addition to this spectral clue, the effect of sample heating was obvious when the sample was visually examined since a small hole could be seen surrounded by charred material.

In dispersive Raman spectroscopy, there is no obvious equivalent to the black-body radiation tail to serve as an indicator of sample heating. However, the majority of solid samples that strongly absorb radiation show the effect of catastrophic sample heating (burning, or charring). The appearance of bands related to amorphous carbon is an indicator of catastrophic sample heating in the spectrum. The appearance of bands due to carbon can be seen in the Raman spectra of samples measured with lasers from the NIR to the UV. For UV excitation, the radiation is so energetic that even very low laser powers can cause

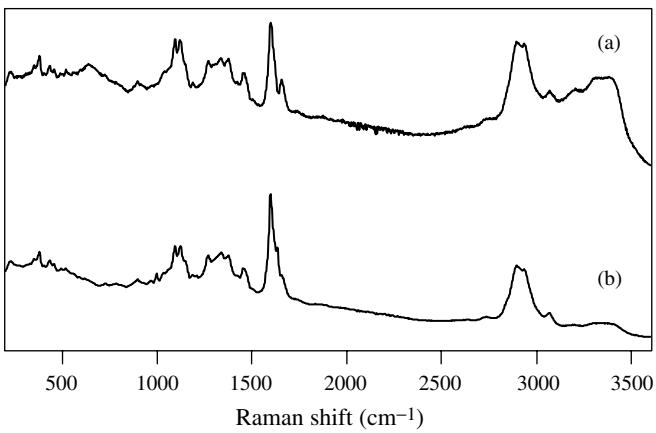

Figure 17. FT-Raman spectrum of lodgepole pine measured with a laser power of (a) 750 mW and (b) 400 mW. [Reproduced from Lewis *et al*. (1994).[43]]

Handbook of Vibrational Spectroscopy, Online © 2006 John Wiley & Sons, Ltd.

This article was published in the *Handbook of Vibrational Spectroscopy* in 2006 by John Wiley & Sons, Ltd.
DOI: 10.1002/9780470027325.s3103

significant carbon formation in solid samples ranging form biological materials to polymers.

In dispersive Raman microscopy the irradiated area is small in comparison to the spot in an FT-Raman spectrometer (up to two or three orders of magnitude smaller). Thus even though the laser power of the diode laser is smaller than the Nd : YAG the power per unit area of the dispersive Raman microprobe is not insignificant. In Raman microscopy it is not uncommon to heat a polymer sample and cause it to curl up and move out of the focus. This does not lead to an artifact in the spectrum but does lead to a spectrum with a lower S/N than anticipated.

Sometimes it is possible to change the heat capacity of the surroundings or to use the surrounding material as a heat sink to increase the rate of heat flow from the sample and allow the Raman spectrum to be collected. One simple solution to this problem when the sample is a powder is simply to prepare it as a mull in a mineral oil such as Nujol®. The majority of the dissipation of thermal radiation in this case is due to the contact of the sample with the salt plate and not the Nujol®.[44] An advantage to this approach is that the sample can be mixed with the same sample-to-Nujol® concentration that would be appropriate for infrared transmission spectroscopy. Hence, using the same sample holder one can collect both the Raman and infrared spectrum. A drawback to this approach, however, for weak Raman scatters is that the presence of the Nujol® oil will lead to the appearance of Raman bands due to Nujol® in the spectrum of the sample and possible self-absorption by Nujol® (see Section 3.4). As long as these bands appear outside the spectral range of interest then this is not a problem.

As noted above it is the contact between the sample and the KBr salt plates that allows the dissipation of the thermal energy; one would conclude that a KBr disk (similar to that traditionally used in infrared spectroscopy) would be the most effective medium. The success of this approach was demonstrated by West using several different inorganic compounds known to have difficulties with laser-induced heating.[39] Another way to further increase the heat flow is to grind the particle up more finely. The smaller particles would have more surface area that could dissipate the radiation, and smaller particles give rise to stronger Raman signals.[38]

In another example,[45] an aromatic nitrated explosive 1,4,5,8-tetranitronaphthalene (TNN) was examined using a FT-Raman spectrometer. In this example, the loosely packed sample was held in a sample cup and the spectrum obtained (Figure 18a). In Figure 18(b) the spectrum of the same explosive is again shown but this time the sample was packed into the sample cup. The two spectra are obviously different in the range 3600 to 2500 cm^{-1}. This example is provided as a warning, since the level of sample heating is not very great. In fact with mild sample heating of an unknown sample, the elevated baseline and shape in the range 3600 to 2500 cm^{-1} might be interpreted as indications of the presence of NH and aliphatic CH. In fact, for the example shown here, TNN contains neither of these functional groups. Grinding and sample packing are not universal solutions to the problems of sample heating, however. Some samples form glassy surfaces after packing, while some pharmaceuticals may undergo polymorphic changes.

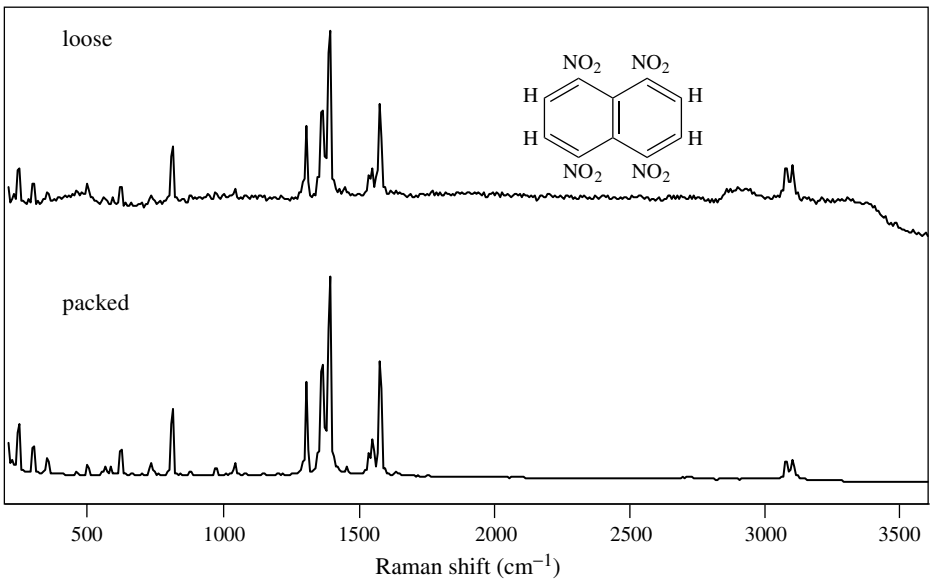

Figure 18. Raman spectrum of the explosive TNN, measured as (a) a loose powder and (b) packed. [Reproduced from Lewis *et al.* (1995).[45]]

DOI: 10.1002/9780470027325.s3103

Another solution proposed for sampling heating is demagnification of the focused laser beam to distribute the total laser power over a larger area of the sample, although there is not a provision to defocus the spot for most FT-Raman spectrometers. In this case, the sample may be simply moved away from the beam focus; it should be noted, however, that this is done at the expense of total collected signal (especially for reflective based optics[20]). In dispersive Raman equipped with microscopes, several approaches are available for defocusing the spot at the sample but care must be taken to adopt an approach which will not significantly degrade the collection efficiency.

Cooling the sample using a cryogenic cold finger is another way of avoiding excessive sample heating. In this case, the sample is held in a tube and the tube is cooled to 77 K. In this approach the heating rate of the sample is anticipated to be lower or at least equal to the cooling rate of the sampling accessory. An example of this approach is shown in Figure 19 where the spectrum of tris(triphenylphosphine) cobalt chloride is shown.[46] It had been found to be impossible to measure the spectrum of an uncooled sample of this material with 1064-nm excitation or with visible excitation and a CCD-based spectrometer. This approach has its drawbacks as well since the sample must fit in the apparatus, the sample may change its state on cooling, and ice formation may occur.[4]

Two more approaches that are specific to FT-Raman spectrometry have been proposed. The first is only applicable to samples that undergo mild sample heating. In this approach, sample heating is allowed to occur but the black-body thermal emission is blocked prior to reaching the interferometer using a short-pass filter. The short-pass filter blocks radiation at Raman shifts greater than 2000 cm^{-1} (7400 cm^{-1} absolute). The result of this approach is to increase the S/N of the sample Raman spectrum in the range 100–2000 cm^{-1} by reducing multiplex noise and background from the black-body tail. The second approach is to couple a pulsed laser and special detection to the FT-Raman spectrometer. Several reports of the use of either a Q-switched pulsed Nd : YAG laser[46,47] or a synchronously gain-switched Nd : YAG laser[48,49] along with special detection techniques have appeared that lead to efficient rejection of thermal backgrounds. Despite the initial promise of this work, this approach has, to the time of this writing, not been commercialized, probably because of a combination of instrument complexity and expense.

Finally it is sometimes possible to spin the sample to reduce the effect of heating. (This will be discussed in detail in a later section.)

3.3 Fluorescence

While it is generally true to say that the fluorescence of organic molecules is a less serious problem for FT-Raman than CCD-Raman spectrometry, it is certainly not true to say that fluorescence is never a problem in FT-Raman spectrometry. For example, the spectrum of a black ceramic product is shown in Figure 20. There is no possibility of observing any Raman bands above the fluorescent background in this case.

Many techniques have been explored to remove the effect of fluorescence from Raman spectra. Most of them exploit the fact that fluorescence intensity changes very slowly across the spectrum, so that the elevated baseline that is typically caused by fluorescence may be removed by software after the measurement. Most commonly, a simple baseline correction routine is applied. Alternatively, the first or second derivative of the spectrum may be calculated. The same effect can also be achieved by subtracting two spectra

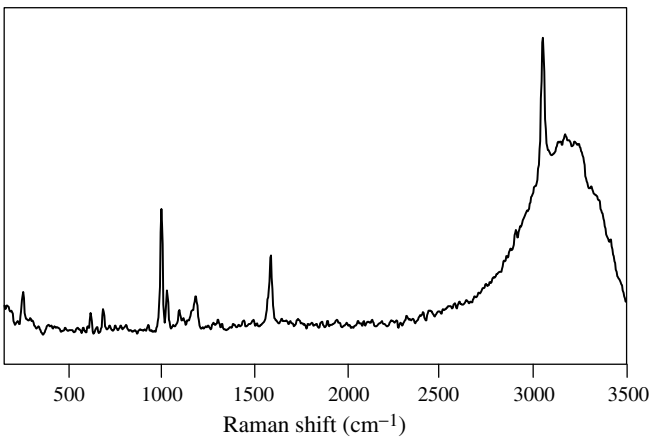

Figure 19. FT-Raman spectrum of tris(triphenylphosphine) cobalt chloride in a tube that was cooled to 77 K. [Reproduced from Edwards *et al*. (1994).[46]]

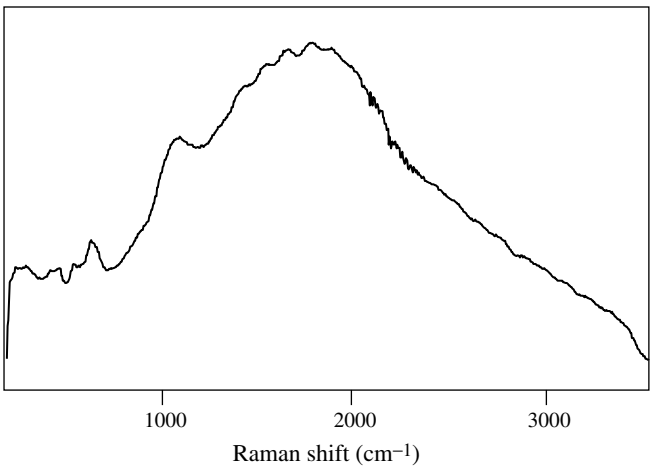

Figure 20. FT-Raman spectrum of a strontium-doped $BaTiO_3$ ceramic.

DOI: 10.1002/9780470027325.s3103

of the same sample measured with laser wavelengths that are different by about $10\,cm^{-1}$. Since the fluorescent emission remains at the same absolute wavenumber while the absolute wavenumber of the Raman bands changes by the amount that the laser frequency is shifted, the first derivative of the spectrum will result.[50] Unfortunately this technique requires access to a tunable laser, which is rarely supplied with most Raman spectrometers. No matter whether the effect of fluorescence is minimized by software or hardware, however, the increase in shot noise that is derived from the high intensity of light that is incident on the detector degrades the spectrum significantly.

An alternative technique makes use of the fact that Raman scattering is effectively instantaneous while fluorescent emission takes place over a nanosecond timescale. For example, Matousek *et al*.[51] described how a Kerr gate could be used to reject most of the radiation due to fluorescence. It should be noted, however, that the number of photons emitted by fluorescence is greatest immediately after the excitation pulse is absorbed, so time gating can never completely eliminate the effects of fluorescence. Furthermore, this method requires picosecond time resolution; thus time gating is neither trivial nor inexpensive.

It is obviously more beneficial to use a laser wavelength that is long enough that no fluorescence is generated. As noted earlier, the need to eliminate, or at least minimize, fluorescence is what has led to the current popularity of NIR Raman spectroscopy. Even the 1064-nm radiation from a Nd : YAG laser is not of long enough wavelength to eliminate fluorescence from all organic samples, however, and Asselin and Chase[52] have shown an example of where the Raman spectrum of a highly fluorescent sample could only be obtained with the 1300-nm line from a Nd : YAG laser.

The problems encountered with organic samples pale into insignificance when compared with those found with certain inorganic samples. For example, we were attempting to measure the FT-Raman spectrum of a ceramic powder that was largely composed of barium titanate using a Nd^{3+} : YAG laser. A spectrum was easily measured (Figure 21a). Because the measurement of Raman spectra is now so quick and easy, we also measured the spectrum on a CCD-Raman spectrometer equipped with a 785-nm laser (Figure 21b). We were surprised that the spectra were totally different. Obviously many of the features in the FT-Raman spectrum were actually artifacts. We believe that they are caused by sharp luminescence bands from trace lanthanide ions that were present in the sample. Because the width of these bands was of the same order as the Raman bands, they could not be eliminated by calculating the first derivative of the spectrum. Furthermore, since luminescence is generally increased when the excitation wavelength is reduced, one would expect that at least

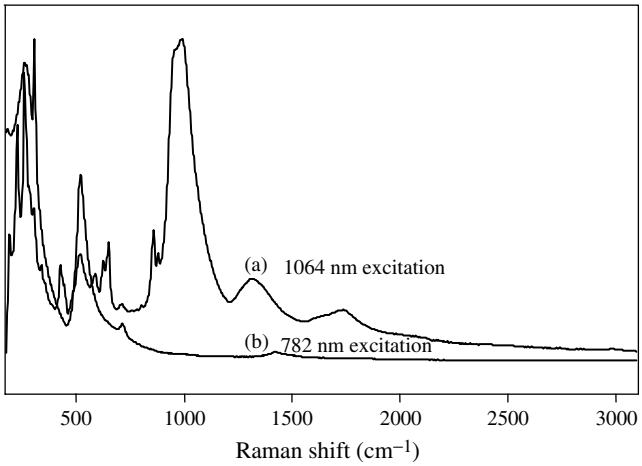

Figure 21. Narrow band fluorescence. (a) Spectrum of $BaTiO_3$ measured on an FT-Raman spectrometer; (b) spectrum of the same $BaTiO_3$ sample measured on a CCD-Raman spectrometer.

some of the bands in the spectrum measured with 785-nm excitation are due to luminescence derived from trace lanthanide ions.

It is well known that any band that is seen in the Stokes-shifted Raman spectrum must be present in the corresponding anti-Stokes spectrum. The notch filters that are installed in all modern Raman spectrometers to eliminate the Rayleigh line are generally fabricated so that they only eliminate a small part (typically about $100\,cm^{-1}$) of the Stokes Raman spectrum and are not as efficient for the anti-Stokes side of the spectrum. Nonetheless, we were able to measure a reasonably good anti-Stokes spectrum of the sample with 785-nm excitation. The Stokes and anti-Stokes spectra are plotted in Figure 22. It can be seen

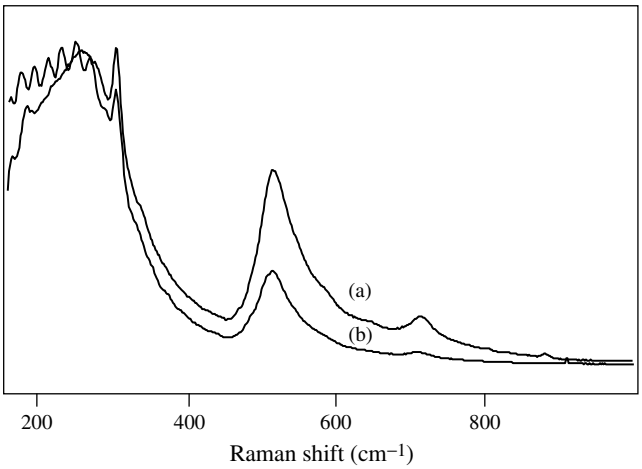

Figure 22. Fluorescence rejection. (a) CCD-Raman Stokes shifted spectrum of $BaTiO_3$; (b) CCD-Raman spectrum of the anti-Stokes shifted spectrum. Because the instrument response was not corrected for, there are undulations below $250\,cm^{-1}$ in the anti-Stokes shifted spectrum due to interference fringes of the holographic notch filter.

DOI: 10.1002/9780470027325.s3103

that the bands around 300, 500 and 700 cm^{-1} Raman shift are present in both the Stokes and anti-Stokes spectrum, indicating that they are Raman bands and were not caused by luminescence. We have observed similar luminescence bands when measuring the spectra of other "real-world" inorganic samples such as bricks and porcelain ceramics, although these bands were usually broader than the ones shown in Figure 22. Although broadband luminescence from transition metals has been described by Sugano *et al*.[53] and reported in Raman spectra,[38,54–56] the bands shown in Figure 19 are much narrower than those from transition metals, increasing the possibility of confusing them with Raman bands.

Sometimes the Raman spectra of lanthanide salts can be exceptionally difficult to obtain. For example, the spectrum of neodymium phosphate measured on an FT-Raman spectrometer equipped with a 1064-nm Nd : YAG laser and both the Stokes and anti-Stokes shifted spectra measured on a CCD-Raman spectrometer equipped with a 785-nm diode laser are shown in Figure 23. None of the spectral features in the "Raman spectrum" of neodymium phosphate measured in one way matches the features in the spectra measured in the other two ways. It is quite possible that there is a resonance effect for both excitation wavelengths but it is definitely unclear as to which bands are true Raman bands of neodymium phosphate. Other lanthanides such as holmium oxide, ytterbium oxide, ytterbium sulfide and praseodymium nitrate have also exhibited similar phenomena. Thus measuring the anti-Stokes spectrum is not a universal solution. Since the lifetime of the excited states of lanthanides can be quite long, it is possible that time gating would prove to be an effective, albeit expensive, way of eliminating these bands.

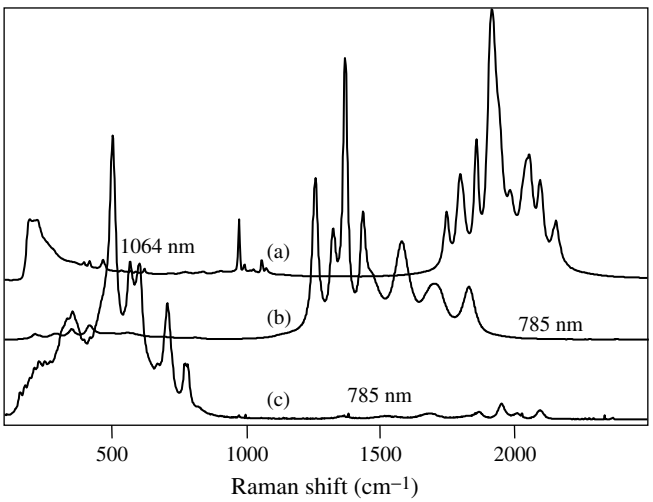

Figure 23. Elucidation of true Raman bands (see text for details). (a) FT-Raman Stokes shifted spectrum of neodymium phosphate; (b) CCD-Raman Stokes shifted spectrum of neodymium phosphate; (c) CCD-Raman anti-Stokes shifted spectrum of neodymium phosphate.

As expected, the relative intensities of the bands in the anti-Stokes and Stokes spectra decrease with increasing Raman shift (Figure 23). This is because the bands in the anti-Stokes spectrum require the excitation of species in the first excited vibrational state and the Boltzmann population of this state decreases as $\tilde{\nu}_{Vib}$ increases. Measuring the anti-Stokes spectrum is a good way to reject luminescence. However, it is difficult to measure anti-Stokes Raman bands of much greater than about 1200 cm^{-1} shift because the Boltzmann population of the vibrational state from which these transitions are derived is too low. A good example of the possible usefulness of measuring anti-Stokes spectra is illustrated by an experiment performed by Iida *et al*.,[57] where the anti-Stokes spectrum was used to monitor a fluorescent reaction of a gel at a temperature of 500 °C. In this case, measuring the anti-Stokes aided in rejecting fluorescence and the effects seen from thermal emission. Not only have anti-Stokes measurements been used to discriminate between electronic and vibrational transitions, but they have also been postulated to be a useful technique to discriminate between fundamental and other vibrational bands such as overtones, combination bands and Fermi-resonance bands.[58]

3.4 Matrix absorption

Raman scattered light generated from within a sample must pass back through the sample before reaching the collection optics. If the Raman spectrum of a liquid is being measured, the Raman-scattered radiation must also pass through the walls of the container. Thus the Raman spectrum of the sample is affected by the transmission characteristics of the sample and sample container. Within a few years of the development of FT-Raman spectroscopy reports appeared on what has become known as self-absorption.[38,59–62] These authors note that for X–H solvents there is an interaction between NIR overtones or combination bands of the solvent and the Raman spectrum, which leads to lower than expected intensities of Raman bands than would be expected. In addition as the concentration of the X–H solvent rises the effect can become greater which could lead to problems in quantitative Raman measurement of solute concentration.

To illustrate the effect of matrix absorption on the relative intensities of Raman bands, let us consider the FT-Raman spectrum of acetonitrile. The spectrum of pure acetonitrile is shown in Figure 24(a) and the corresponding spectrum of an acetonitrile : water mixture is shown in Figure 24(b). A large decrease in the intensity of the C≡N stretching band

Handbook of Vibrational Spectroscopy, Online © 2006 John Wiley & Sons, Ltd.

This article was published in the *Handbook of Vibrational Spectroscopy* in 2006 by John Wiley & Sons, Ltd.
DOI: 10.1002/9780470027325.s3103

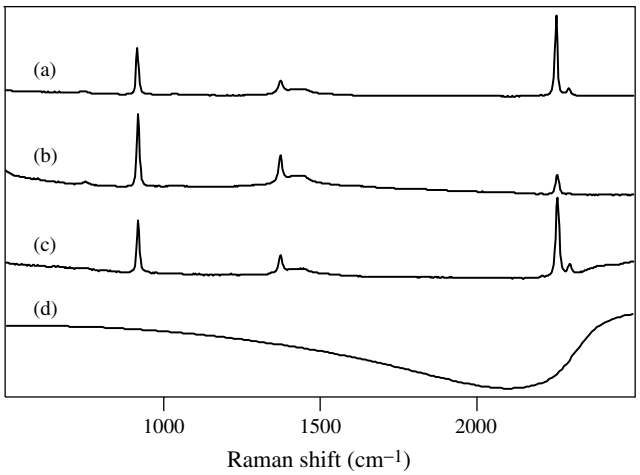

Figure 24. Effect of matrix absorption. (a) FT-Raman spectrum of neat acetonitrile; (b) FT-Raman spectrum of acetonitrile in H_2O; (c) FT-Raman spectrum of acetonitrile in D_2O; (d) transmittance spectrum between 0 and 100% T of a 1-mm path of H_2O from $\sim$8900 cm^{-1} to 6900 cm^{-1} shifted relative to a Nd : YAG at $\sim$9400 cm^{-1}.

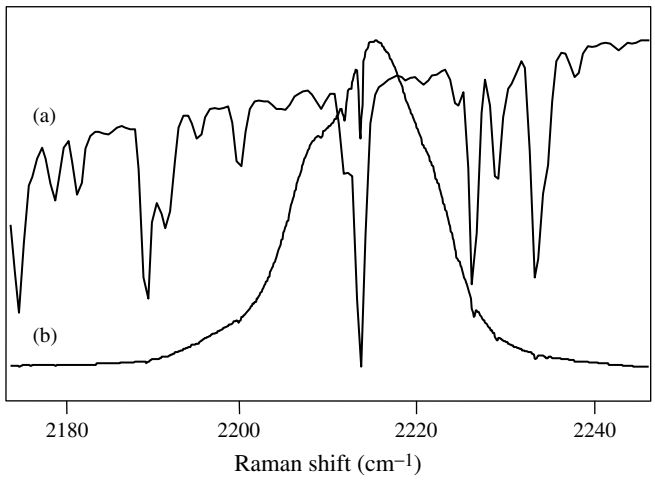

Figure 25. Effect of atmospheric absorption. (a) Transmittance spectrum of water vapor adjusted to Raman shifted units; (b) FT-Raman spectrum of C≡C stretch of a macrocycle containing several C≡C groups in the same spectral region.

near 2250 cm^{-1} (Raman shift) may be seen. This intensity change is not seen in the spectrum of the $CH_3CN : D_2O$ mixture shown in Figure 24(c), indicating that the effect is probably caused by absorption of the Raman scattered radiation by water. The NIR transmittance spectrum of a 10 mm thick sample of water is shown in Figure 24(a), after subtracting the absolute wavenumber from 9398 cm^{-1} so that the wavenumber scale corresponds to that of the Raman spectra shown in this figure. The transmittance of D_2O is significantly greater than that of H_2O in this spectral region, which accounts for the difference between the spectra in Figure 24(b) and (c). Thus the decrease in the intensity of the C≡N stretching band seen in the spectrum of the $CH_3CN : D_2O$ mixture was indeed due to the transmission characteristics of water. Such an effect can also alter the linearity of calibration curves, as shown by Schmidt *et al.*[63]

Absorption of Raman scattered radiation by liquid water was not unexpected. However, the use of a 1064-nm excitation laser unearthed an unexpected problem because of absorption by atmospheric water vapor.[38] The C≡C stretching band in the Raman spectrum of a polyacetylene appeared to exhibit fine structure across this band as shown in Figure 25. At first we believed that there were several bands contained within this band, possibly caused by a combination of crystal splitting and the existence of several C≡C groups in different chemical environments. When the NIR transmission spectrum of water vapor was overlaid with the measured spectrum, it became apparent that the "fine structure" was in fact caused by the absorption of the Raman-scattered radiation by atmospheric water vapor. A similar phenomenon can be seen from a 785-nm CCD-spectrometer when the sample optic is pointed towards the sky. For example, Pelletier[64] presented a spectrum which clearly showed Fraunhofer lines and molecular absorptions from the atmosphere.

Both self-absorption and scattering can alter the apparent concentration that is measured from the intensity of a given Raman band since both effects limit the depth beyond the surface of the sample one can probe and still be able to measure a recognizable Raman spectrum.[38,62] This could limit the maximum observable intensity in the spectrum and affect the depth into the sample from which the Raman signal may be observed.[65] For samples with an absorptivity larger than a certain value, the depth into the sample or maximum signal observed is limited by the self-absorption of the sample, whereas for samples with smaller absorptivities the measured signal is limited by the optics of the system.[65]

It should be noted that as the excitation wavelength is shortened the effect of nonresonant self-absorption decreases (as the intensity of the NIR overtones and combination bands decreases). For most applications with 785-nm excitation self-absorption is not a significant problem but for certain sample arrangements when very long pathlength cells (for example liquid core-optical fibers with an effective pathlength of meters) are used, solvent self-absorption can be a problem even with 785-nm excitation.[66,67]

4 SAMPLING

4.1 Introduction

In this section some artifacts, which originate due to sampling, will be discussed. One factor which will not be

DOI: 10.1002/9780470027325.s3103

considered in depth, but which could lead to erroneous results, is contamination due to sample preparation. For example in Raman microscopy micron-sized samples may be analyzed. If the sample is prepared in any way then the possibility of contamination exists. Since this problem is not specific to Raman spectroscopy it will not be discussed further.

4.2 Ambient lighting

In Section 3.4, the problem of water vapor absorption by the air was discussed. In addition to the environment giving rise to absorption bands it is also possible for the environment to give rise to emission features. Both fluorescent lights (sharp lines) and incandescent lights (broad elevated background) can cause problems when measuring Raman spectra unless provisions are made.

Due to the compactness of dispersive Raman systems and the development of fiber coupled Raman probes, Raman analyzers have been adopted for process control application, as described by Everall (**Process Measurements by Raman Spectroscopy**) and Lewis.[68] In Figure 26, the Raman spectrum of molten polypropylene recorded with 532-nm radiation is shown. The spectra measured on-line agreed with the published literature for polypropylene with the exception of the band at 490 cm^{-1} from the 532-nm laser.[68] The feature at 490 cm^{-1} is related to a mercury emission line at 546.0 nm which originates from the fluorescent room lights. Such features are generally easily recognized because of their sharpness and symmetry. Several shielding methods can be employed to minimize the amount of room light measured. These include pointing the fiber probe downwards away from light sources, locating the analysis point to a "naturally" shaded position (making use of existing equipment to provide shade), and adding a light blocking shroud to the area around the analysis point. In the laboratory a light tight Class 1 laser enclosure may be employed.

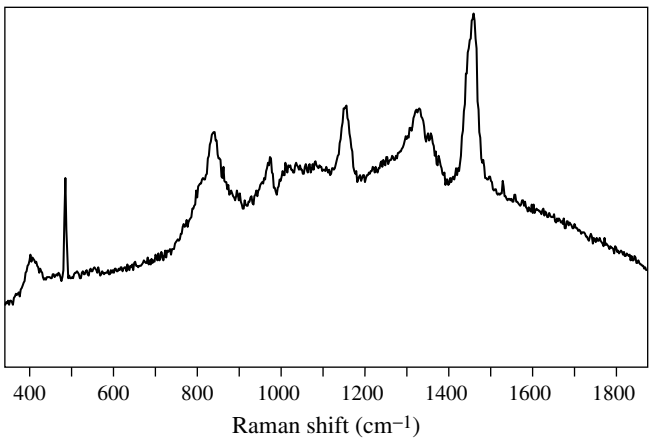

Figure 26. Raman spectrum of molten polypropylene measured with the 532-nm line of a frequency-doubled Nd : YAG laser. The feature at a Raman shift of 490 cm^{-1} is caused by an emission line at 546.0 nm that originates from the fluorescent room lights.

4.3 Air

In the earlier section on sampling heating, mention was made of the use of defocusing to spread out the incident energy on the sample. The simplest way (although not recommended since it can dramatically reduce collection efficiency) of defocusing the laser spot at the sample is to move the sample out of focus. Care should be taken when doing this because in addition to reducing collection efficiency the laser may excite the Raman spectrum of oxygen and nitrogen in the air. In an FT-Raman spectrometer, due to low sensitivity and the low Raman cross-section of gases, it is unlikely that the Q-branch bands for atmospheric oxygen (1555 cm^{-1}) and nitrogen (2330 cm^{-1})[69] would be observed. In CCD-Raman with a Raman microscope even with 785-nm excitation it is possible to measure the Q-branches of oxygen and nitrogen if the sample is out-of focus and long integration times (several minutes) are used. As long as the operator is aware of the presence of these lines, this sampling artifact can be turned to the operator's advantage. The position of these lines can, in fact, be used as calibration monitor to determine if either the wavelength calibration or the laser frequency has changed.

4.4 Sample support surfaces

When a Raman microscope is used to analyze solid samples, the solid is typically mounted on some type of surface to provide support. It is also common for a reflective surface to be placed behind a liquid sample when conducting an FT-Raman analysis.

In these cases artifacts related to the structure or the composition of the support surface may be observed. Barrera and Sommer[65] examined several surfaces, including steel, aluminum, anodized aluminum, etc., and showed that each surface could lead to a different background. Cheng *et al.*[70] have used a silicon wafer as a support surface for their work on explosives. In the spectra measured the distinctive 521 cm^{-1} band related to the first phonon of silicon is observed. In the case of a dielectrically coated mirror if used as the support then, for transparent, weak scatters, the spectrum of titanium dioxide (a constituent of the dielectric stack) can be seen at low frequencies.

In summary, if a support surface is required, a good quality front surface mirror may be employed but the background from the mirror should always be checked.

Handbook of Vibrational Spectroscopy, Online © 2006 John Wiley & Sons, Ltd.

This article was published in the *Handbook of Vibrational Spectroscopy* in 2006 by John Wiley & Sons, Ltd.
DOI: 10.1002/9780470027325.s3103

4.5 Sample containers – glass

One of the attractions of using Raman spectroscopy when compared to infrared spectroscopy is that glass can be used as the optical sample container. In infrared spectroscopy either delicate salt plates or large elemental crystals (such as germanium or diamond) are necessary to provide infrared transparent windows for spectral collection (**Optical Materials for Infrared Spectroscopy**). These elements may be hygroscopic, susceptible to abrasion, susceptible to acid or alkali damage, require precise dimensions, and are expensive. Raman spectroscopy, in principle can be conducted with standard analytical laboratory glassware, such as cuvettes, gas chromatography vials, or NMR tubes. Unfortunately when using NIR excitation, both at 785 and 1064 nm, this statement is an oversimplification. Four points must be taken in consideration when choosing the sample container:

1. thickness and curvature of the container
2. color
3. contaminants
4. material type.

The thickness and curvature will affect both how much light passes to the sample and how the light is focused into/onto the sample. If the glass thickness is large in comparison to the sample volume then a number of broad peaks related to silica Raman scattering will be observed (a similar background to that seen when using optical fibers for Raman spectroscopy, as described by Lewis and Lewis (**General Introduction to Fiber Optics**). The Raman scattering cross-section of glass is weak but may be significant when analyzing weak Raman scatters such as catalysts. It should be noted that the intensity of the silica Raman peaks will depend on the actual position of the focal cylinder with respect to the sample and the container. For example for a liquid the focus is likely to be well inside the walls of the sample vessel; however, for an opaque solid, or a liquid exhibiting self-absorption, the focus will essentially be at the solid/container interface. The reader is referred to the article in this Handbook by McCreery (**Photometric Standards for Raman Spectroscopy**) and to McCreery's book[71] for further information on the effects of the spectrometer depth of field on the measurement.

The color of the glass is also important. Some samples, which may be encountered are photosensitive and are thus stored in brown glass bottles. These vials, which appear to transmit in the visible spectral range, may absorb light in the NIR.

Glass itself is a complex semi-solid material, which can be manufactured in a number of different ways. If the glass material, as is often the case, contains inorganic contaminants then these contaminants may either fluoresce or absorb when excited with NIR radiation (in the same way as if they were the sample – previous section). This can, in the extreme, preclude the observation of sample Raman bands or limit quantitative accuracy.

In addition it is important to note that a vial that has been used successfully for FT-Raman spectroscopy may not be simply used for 785-nm based CCD-Raman spectroscopy. An example of this is shown in Figure 27 where the 1064-nm FT-Raman spectrum of cocaine hydrochloride (Figure 27a) is shown with the 785-nm spectrum of the cocaine hydrochloride (Figure 27b). The background from the vial is clearly seen over the range 1000 to 2200 cm^{-1}. When a spectrum of an empty part of the vial was measured and scale-subtracted, followed by baseline correction then the true Raman spectrum could be observed (Figure 27c). Note that in this study neither the FT-Raman nor the CCD-Raman spectrometers were intensity axis corrected. If the sample container is made of a polymer instead of glass then Raman scatter from the container itself may become the dominant artifact. Scaled spectral subtraction again may be necessary.

In conclusion it can be seen that it is important to either analyze an empty sample container prior to adding the sample to identify sample container problems or to select a "glass" material, which is free of these problems (such as optical grade quartz).

This type of anomaly can be observed in dispersive Raman microscopy for very weak Raman scatters when the scattering from the sample approaches the level of scatter coming from the focusing lens. In most commercial Raman microprobes a trade-off between signal-collection

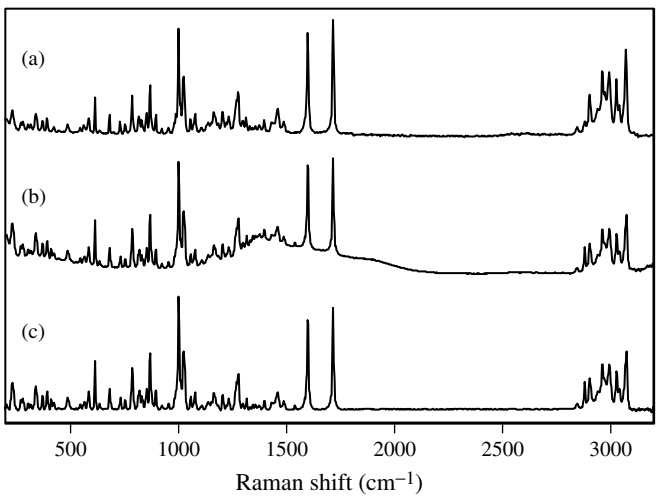

Figure 27. (a) FT-Raman spectrum of cocaine hydrochloride measured with a 1064-nm Nd : YAG laser; (b) CCD-Raman spectrum of the same sample measured with a 785-nm diode laser; (c) result of the scaled subtraction of the spectrum of an empty part of the vial from (b).

DOI: 10.1002/9780470027325.s3103

efficiency (numerical aperture, NA), lens background and cost is often made.

4.6 Sample movement

Samples that slowly heat during analysis can be mounted in a sample spinner. In this arrangement, the sample is rotated in such a manner that the laser only impinges on a particular area of the sample for a small time. This approach has the benefit of sampling more surface area and thus the measured spectrum is a closer representation of the bulk than for a single point measurement. This approach has been successfully employed for CCD-Raman using a variety of excitation wavelengths; however, it is generally inappropriate for FT-Raman spectroscopy because periodic oscillations in the signal caused by high-speed cell rotation can be Fourier-transformed into an artifact sometimes termed spinning side-bands. Solutions to this problem include high precision cells,[72] very slow speed rotation (60 rpm)[73] and step-scan operation of the interferometer.[74]

Similarly, if the sample moves in and out of focus of an FT-Raman spectrometer during the analysis of, for example, a polymer film or fiber in production or if the sample is bubbling then artifacts can also be introduced. These artifacts originate in a similar manner to sample spinning artifacts and can be characterized as periodic oscillation in the spectrum, noise spikes, and increased multiplex noise.[75] These artifacts have contributed to the poor acceptance of FT-Raman spectrometry as an on-line process control tool and has limited these spectrometers to laboratory measurements. Because CCD detectors integrate the signal, CCD-Raman spectrometers do not suffer from these effects.

4.7 Confocal depth analysis

This anomaly relates to the use of Raman microscopy for "depth profiling", "z-scanning", or "optical sectioning" and is independent of the excitation wavelength. Since confocal Raman microscopy, and in general Raman microscopy, is rarely conducted with an FT-Raman spectrometer this anomaly is of more consequence to CCD-Raman spectrometer users.

Raman microscopy has developed as a technique since it offers a unique combination of nondestructive analysis, high spatial resolution, and rich sample characterization information, as described in the book by Turrell *et al.*[76] and the article by Dhamelincourt in this Handbook (**Raman Microscopy**). The spatial resolution of the instrument, however, will be degraded if the sample scatters the excitation and Raman scattered radiation. If an aperture is placed at the back-focal image plane then, in principle, only the radiation emitted from the diffraction-limited laser focal volume will be collected. This approach thus appears very attractive for measuring materials buried in a matrix in a noncontact, nondestructive manner. For example, by first focusing the laser on the sample surface and then moving the microscope stage so that the beam is focused below the surface, information may be obtained on the depth at which an impurity is measured or the thickness of a layer in, for example, a polymer laminate. In commercial Raman instruments, dry metallurgical objectives are commonly used since they provide both high NA, and allow noncontact sampling. Unfortunately these objectives lead to refraction effects when the diffraction limited laser spot is focused through the air/sample interface. This leads to "smearing" of the excitation focal cylinder and a degradation of the confocal performance of the Raman microscope.

Everall[77,78] has developed a model to show the effect of refraction on the Raman experiment and to demonstrate experimentally the effects of excitation focal cylinder "smearing" on measured samples. The results of this model show that, for a high magnification, high NA dry metallurgical objective, the measured layer thickness or depth can be underestimated by approximately a factor of 2. For very high NA objectives, such as 0.95, $\times 100$, the effect is more pronounced than for a 0.75, $\times 50$ objective. In addition, since the focal cylinder is elongated, pure spectra from buried layer may not be measured. Everall[78] further demonstrated that with the use of an immersion objective with approximate (but not perfect) index matching fluid surrounding the objective and the sample the effect of refraction could be minimized. In this arrangement much more accurate intensity vs depth results could be produced. For buried layers it was shown that due to the use of an immersion objective and index matching fluid, the size of the focal cylinder could be reduced and the layer-to-layer contamination for buried layer was reduced (but not eliminated).

In addition to studying the effect of refraction on the excitation side of the experiment, Everall[78] noted that when refraction occurs the confocal aperture had little effect on improving the depth resolution. Baldwin *et al.*[79] have developed a model to show that the confocal aperture is significant when the sample of interest is buried deeply in the matrix (for example in a diamond anvil cell).

These reports show that quantitative confocal depth profiling and profile interpretation are not trivial. The use of immersion objectives and index matching fluid is recommended to prevent anomalous depth/thickness results from being generated. Qualitative depth analysis may be undertaken if the aim of the study is to show the presence of multiple layers; however, structural interpretation of the layers remains difficult due to layer-to-layer contamination.

Handbook of Vibrational Spectroscopy, Online © 2006 John Wiley & Sons, Ltd.

This article was published in the *Handbook of Vibrational Spectroscopy* in 2006 by John Wiley & Sons, Ltd.
DOI: 10.1002/9780470027325.s3103

Scaled subtraction of surface layers or chemometric analysis may enhance interpretability.[80,81]

4.8 Polarization

The final artifact which will be discussed brings us back full circle to Raman's early reports[1,2] and his first report on the effect of polarization on Raman spectra. The measured Raman spectra of many samples is highly dependent on the orientation of the sample and the polarization properties of the laser and spectrometer. Each optical component in the experimental set-up can play a part – for example, polarization scrambling from mirrors or Woods anomalies in reflective diffraction gratings.[13] In many experimental set-ups, calcite polarizers are used to define the polarization state of the beam that is passed to the sample or the detector. Inaccurate results can be measured if the polarizing element itself is not flat, perpendicular to the incoming beam, or rotation is not perfectly reproducible. As the popularity of Raman microscopes based on CCD detection has increased, more and more polarization work is being attempted with these types of instruments. Under these conditions if the focusing objective is not careful selected erroneous results can be obtained. Everall[82] has shown that P_{lmn} order parameters, which can be related to quantitative orientation information in polymer films and fiber, can be significantly underestimated when a high NA (0.95, $\times$100) objective was used while a lower NA (0.75, $\times$50) objective gave good results. These results were explained by Everall on the basis of work by Turrell[83] as "effective depolarization of the light field within the focal volume of the high-NA lens".

5 SUMMARY

The aim of this article has been to summarize the origin of artifacts and anomalies in Raman spectra. Many of the effects described can be completely avoided by using good experimental design. As Raman instrumentation is adopted more widely, in both industry and academia, it becomes increasingly important that the problems that may be encountered are recognized and their solutions become well known. It should be stressed that it is usually very easy to measure the Raman spectrum of most organic samples using either a FT or CCD Raman spectrometer equipped with a laser emitting in the NIR. There are samples and application areas which have benefited tremendously from the development of small compact lasers in the visible and the development of UV-excited Raman spectroscopy (for example the thin-film and semiconductor areas). Both UV and NIR excitation are relatively new wavelengths for Raman spectroscopy and as their popularity continues to increase, more samples will undoubtedly be found where these, and other as yet undiscovered, phenomena will be encountered.

ACKNOWLEDGMENTS

Note that some of this article was originally published in two articles in *Applied Spectroscopy (Appl. Spectrosc.*, **54**, 164A, 200A (2000)). The permission of the Society for Applied Spectroscopy to reproduce this material is gratefully acknowledged.

ABBREVIATIONS AND ACRONYMS

MSB	Methyl Styryl Benzene
QE	Quantum Efficiency
TNN	1,4,5,8-Tetranitronaphthalene

REFERENCES

1. C.V. Raman and K.S. Krishnan, *Nature*, **121**, 501 (1928).
2. C.V. Raman and K.S. Krishnan, *Proc. R. Soc. London*, **122**, 23 (1929).
3. D.A. Long, 'Raman Spectroscopy', McGraw-Hill, New York (1977).
4. D.A. Long, *Int. Rev. Phys. Chem.*, **7**, 314 (1988).
5. T. Hirschfeld and B. Chase, *Appl. Spectrosc.*, **40**, 133 (1986).
6. D.B. Chase and J.F. Rabolt (eds), 'Fourier Transform Raman Spectroscopy', Academic Press, New York (1994).
7. S.B. Dierker, C.A. Murray, J.D. Legrange and N.E. Schlotter, *Chem. Phys. Lett.*, **137**, 453 (1987).
8. D.N. Batchelder, *Eur. Spec. News.*, **80**, 28 (1988).
9. Y. Wang and R.L. McCreery, *Anal. Chem.*, **61**, 2647 (1989).
10. J.M. Williams, R.L. Bolling and R.L. McCreery, *Appl. Spectrosc.*, **43**, 372 (1989).
11. S.M. Angel and M.L. Myrick, *Anal. Chem.*, **61**, 1648 (1989).
12. S.M. Angel, M. Carrabba and T.F. Cooney, *Spectrochim. Acta*, **51A**, 1779 (1995).
13. J.-Y. Staff, 'Handbook of Diffraction Gratings, Ruled and Holographic', Longjumeau, France (1980).
14. J.M. Tedesco, H. Owen, D.M. Pallister and M.D. Morris, *Anal. Chem.*, **65**, 441A (1993).
15. R.V. Burch, US Patent 5 247 343 (1993).
16. S. Svanberg, 'Atomic and Molecular Spectroscopy: Basic Aspects and Practical Applications', Springer-Verlag, Berlin (1992).
17. S.D. Smith, 'Diode-laser-pumped Solid-state Lasers', in "Optoelectronic Devices", Prentice Hall International, Hemel Hempstead, 257–283 (1995).

This article was published in the *Handbook of Vibrational Spectroscopy* in 2006 by John Wiley & Sons, Ltd.
DOI: 10.1002/9780470027325.s3103

18. B.T. Bowie and P.R. Griffiths, *Appl. Spectrosc.*, **53**, 1192 (2000).
19. J.R. Birch and F.J.J. Clarke, *Anal. Chim. Acta*, **380**, 369 (1998).
20. D.J. Cutler, *Spectrochim. Acta*, **46A**, 131 (1990).
21. P.R. Griffiths and J.A. de Haseth, 'Fourier Transform Infrared Spectrometry', Wiley Interscience, New York (1986).
22. S.F. Parker, N. Conway and V. Patel, *Spectrochim. Acta*, **49A**, 657 (1993).
23. J.B. Slater and J.M. Tedesco, US Patent 6 067 156 (2000).
24. F.S. Allen, J. Zhao and D.S. Butterfield, US Patent 6 141 095 (2000).
25. K. Lepla and G. Horlick, *Appl. Spectrosc.*, **44**, 1259 (1990).
26. C. Shen, T.J. Vickers and C.K. Mann, *Appl. Spectrosc.*, **52**, 772 (1992).
27. H.S. Carman, Jr, D.C. Alsmeyer, C.H. Juarez-Gracia, A.G. Garrett, B.E. Wilson and V.A Nicely, US Patent 5 850 632 (1998).
28. J.M. Tedesco and K.L. Davis, *Proc. SPIE*, **3537**, 200 (1998).
29. J.G. Radziszewski and J. Miehl, *Appl. Spectrosc.*, **44**, 414 (1990).
30. R.L. McCreery, 'CCD Aray Detectors for Multichannel Raman Spectroscopy', in "Raman Spectroscopy in Charge-transfer Devices in Spectroscopy", eds J.V. Sweedler, K.L. Ratzlaff and M.B. Denton, VCH Publishers, Weinheim, 227–279 (1994).
31. T. Hirschfeld, *Appl. Spectrosc.*, **30**, 68 (1976).
32. J.M. Harnly and R.E. Fields, *Appl. Spectrosc.*, **51**, 334A (1997).
33. W. Hill and D. Rogalla, *Anal. Chem.*, **64**, 2575 (1992).
34. H. Takeuchi, S. Hashimoto and I. Harada, *Appl. Spectrosc.*, **47**, 129 (1993).
35. D.J. Cutler, H.M. Mould, B. Bennett and A.J. Turner, *J. Raman Spectrosc.*, **22**, 367 (1991).
36. A. Schulte, T.J. Lenk, V.M. Hallmark and J.F. Rabolt, *Appl. Spectrosc.*, **45**, 325 (1991).
37. H.M.M. Wilson, M.V. Pellow-Karman, B. Bennett and P.J. Hendra, *Vib. Spectrosc.*, **10**, 89 (1996).
38. B. Schrader, A. Hoffmann and S. Keller, *Spectrochim. Acta*, **47A**, 1135 (1991).
39. Y.D. West, *The Internet Journal of Vibrational Spectroscopy*, **1**, 1 (1996).
40. N.J. Everall, J. Lumsdon and D.J. Christopher, *Carbon*, **29**, 133 (1991).
41. N. Everall and J. Lumsdon, *J. Mater. Sci.*, **26**, 5269 (1991).
42. M.J. Pelletier, *Appl. Spectrosc.*, **53**, 1087 (1999).
43. I.R. Lewis, N.W. Daniel, Jr, N.C. Chaffin and P.R. Griffiths, *Spectrochim. Acta*, **50A**, 1943 (1994).
44. G. Dent, *Spectrochim. Acta*, **51A**, 1975 (1995).
45. I.R. Lewis, N.W. Daniel, Jr, N.C. Chaffin, P.R. Griffiths and M.W. Tungol, *Spectrochim. Acta*, **51A**, 1985 (1995).
46. H.G.M. Edwards, I.R. Lewis and P.H. Turner, *Inorg. Chim. Acta*, **216**, 191 (1994).
47. C.J. Petty and R. Bennett, *Spectrochim. Acta*, **46A**, 331 (1990).
47. D.J. Cutler and C.J. Petty, *Spectrochim. Acta*, **47A**, 1159 (1991).
48. R. Bennett, *Spectrochim. Acta*, **50A**, 1813 (1994).
49. R. Bennett, *Spectrochim. Acta*, **51A**, 2001 (1995).
50. A. Shreve, N.J. Cherepy and R.A. Mathies, *Appl. Spectrosc.*, **46**, 707 (1992).
51. P. Matousek, M. Towrie, A. Stanley and A.W. Parker, *Appl. Spectrosc.*, **53**, 1485 (1999).
52. K. Asselin and B. Chase, *Appl. Spectrosc.*, **48**, 699 (1994).
53. S. Sugano, Y. Tanabe and H. Kamimura, 'Multiplets of Transition Metal Ions in Crystals', Academic Press, New York (1970).
54. A. Mortensen, D.H. Christensen, O.F. Neilson and E. Pedersen, *J. Raman Spectrosc.*, **22**, 47 (1991).
55. A. Aminzadeh, *Appl. Spectrosc.*, **51**, 817 (1997).
56. E. Zhou, S. Bhaduri, S.B. Bhaduri, I.R. Lewis and P.R. Griffiths, 'Auto Ignition Processing of Nanocrystalline Zirconia', in "Processing and Properties of Nanocrystalline Materials", eds C. Suryanarayana, J. Singh and F.H. Froes, The Materials, Mines, and Metallurgy Society, Cleveland, OH, 123–133 (1996).
57. Y. Iida, M. Furukawa, K. Kato and H. Morikawa, *Appl. Spectrosc.*, **51**, 673 (1997).
58. R.J. Meier and A. van de Pol, *Vib. Spectrosc.*, **23**, 95 (2000).
59. N. Everall, J. Lumsden, *Vib. Spectrosc.*, **2**, 257 (1991).
60. C.J. Petty, *Vib. Spectrosc.*, **2**, 263 (1991).
61. D.D. Archibald and P. Yager, *Appl. Spectrosc.*, **46**, 1613 (1992).
62. N.J. Everall, *J. Raman Spectrosc.*, **25**, 813 (1994).
63. K.J. Schmidt, S.L. Zhang, K.H. Michaelian, M.A. Webb and G.R. Loppnow, *Appl. Spectrosc.*, **53**, 1206 (1999).
64. M.J. Pelletier, 'Introduction to Applied Spectroscopy', in "Analytical Raman Spectroscopy", ed. M.J. Pelletier, Blackwell Science, Oxford, 32–33 (1999).
65. B.A. Barrera and A.J. Sommer, *Appl. Spectrosc.*, **52**, 1483 (1998).
66. R. Altkorn, I. Koev and M.J. Pelletier, *Appl. Spectrosc.*, **53**, 1169 (1999).
67. B.J. Marquardt, P.G. Vahey, R.E. Synovec and L.W. Burgess, *Anal. Chem.*, **71**, 4808 (1999).
68. I.R. Lewis, 'Process Raman Spectroscopy', in "Handbook of Raman Spectroscopy", eds I.R. Lewis and H.G.M. Edwards, Marcel Dekker, New York, 919–974 (2001).
69. W.F. Murphy, 'Chemical Applications of Gas-phase Raman Spectroscopy', in "Analytical Raman Spectroscopy", eds J.G. Grasselli and B.J. Bulkin, Wiley-Interscience, New York, Chapter 12 (1991).
70. C. Cheng, T.E. Kilbride, D.N. Batchelder, R.J. Lacey and T.G. Sheldon, *J.Forens. Sci.*, **40**, 31 (1995).
71. R.L. McCreery, 'Raman Spectroscopy for Chemical Analysis', John Wiley, New York (2000).

Handbook of Vibrational Spectroscopy, Online © 2006 John Wiley & Sons, Ltd.

This article was published in the *Handbook of Vibrational Spectroscopy* in 2006 by John Wiley & Sons, Ltd.
DOI: 10.1002/9780470027325.s3103

72. S.H.R. Brienne, R.D. Maxwell, S.M. Barnett, I.S. Butler and J.A. Finch, *Appl. Spectrosc.*, **47**, 1131 (1993).
73. P.J. Hendra, *Internet Journal of Vibration Spectroscopy*, **1**, 1 (1996).
74. R. Salzer, U. Roland, R. Born and J. Sawatski, *Appl. Spectrosc.*, **51**, 1471 (1997).
75. G.J. Gervasio and M.J. Pelletier, *At-Process*, **3**, 7 (1997).
76. G. Turrell, M. Delhaye and P. Dhamelincourt, in "Characteristics of Raman Microscopy in Raman Microscopy: Developments and Applications", eds G. Turrell and J. Corset, Academic Press, Inc., San Diego, CA, Chapter 2, 27–49 (1996).
77. N.J. Everall, *Appl. Spectrosc.*, **54**, 773 (2000).
78. N.J. Everall, *Appl. Spectrosc.*, **54**, 1515 (2000).
79. K.J. Baldwin, D.N. Batchelder and S. Webster, 'Raman Microscopy: Confocal and Scanning Near-field', in "Handbook of Raman Spectroscopy", eds I.R. Lewis and H.G.M. Edwards, Marcel Dekker, New York, 145–190 (2001).
80. N.J. Jestel, J.M. Shaver and M.D. Morris, *Appl. Spectrosc.*, **52**, 64 (1998).
81. J.J. Andrew and T.M. Hancewicz, *Appl. Spectrosc.*, **52**, 797 (1998).
82. N.J. Everall, *Appl. Spectrosc.*, **52**, 1498 (1998).
83. G. Turrell, 'Raman Sampling', in "Practical Raman Spectroscopy", eds D.J. Gardiner and P.R. Graves, Springer-Verlag, Berlin, Chapter 2, 13–54 (1989).

Handbook of Vibrational Spectroscopy, Online © 2006 John Wiley & Sons, Ltd.

This article was published in the *Handbook of Vibrational Spectroscopy* in 2006 by John Wiley & Sons, Ltd.
DOI: 10.1002/9780470027325.s3103